1992

In Situ Stress Measurements to 3.5 km Depth in the Cajon Pass Scientific Research Borehole: Implications for the Mechanics of Crustal Faulting

Mark D. Zoback
Stanford University, zoback@stanford.edu

John H. Healy
U.S. Geological Survey

JOURNAL OF GEOPHYSICAL RESEARCH, VOL. 97, NO. B4, PAGES 5039–5057, APRIL 10, 1992

In Situ Stress Measurements to 3.5 km Depth in the Cajon Pass Scientific Research Borehole: Implications for the Mechanics of Crustal Faulting

MARK D. ZOBACK

Department of Geophysics, Stanford University, Stanford, California

JOHN H. HEALY

Office of Earthquakes, Volcanoes and Engineering, U.S. Geological Survey, Menlo Park, California

Measurements of in situ stress orientation and magnitude at the site of the Cajon Pass research borehole have been made from depths of 0.9–3.5 km using the hydraulic fracturing technique and analysis of stress-induced well bore breakouts. The results of these measurements support two important conclusions about the mechanics of crustal faulting. First, the magnitudes of measured in situ stresses indicate ratios of shear to normal stress on favorably oriented fault planes that are consistent with predictions based on Mohr-Coulomb theory and laboratory-determined coefficients of friction in the range of 0.6–1.0 assuming hydrostatic pore pressure (this is commonly known as Byerlee's law). Thus the stress measurements indicate that the frictional strength of the crust adjacent to the San Andreas fault is high (i.e., consistent with laboratory-derived friction values) and that the level of shear stress in the crust adjacent to the San Andreas is principally controlled by its frictional strength. However, data on the orientation of maximum horizontal compression in the borehole from 1.75 to 3.5 km (N57°E ± 19°) indicate that the San Andreas must be quite weak as a complete absence of right-lateral shear stress resolved on planes parallel to the ~N60°W striking San Andreas fault is observed. The lack of right-lateral shear stress on planes parallel to the San Andreas fault at this site is especially surprising as Cajon Pass is located along a section of the San Andreas which has not had a major earthquake since 1812 and is thus presumably quite "late" in the earthquake cycle. Nevertheless, both the orientation and magnitudes of stresses measured in the well are consistent with the style of active faulting in the area surrounding the drill site, most notably normal faulting and Quaternary age left-lateral slip on the Cleghorn fault that parallels the San Andreas in the vicinity of the drill site (Meisling and Weldon, 1982; Weldon, 1986; R. J. Weldon et al., unpublished report, 1981). We argue that the stress state (and Quaternary fault offsets) observed in the Cajon Pass area could exist only if the San Andreas moved at low shear stresses comparable to seismic stress drops rather than the much higher values predicted by Byerlee's law, a conclusion consistent with the lack of frictionally generated heat flow along the San Andreas system (e.g., Brune et al., 1969; Henyey and Wasserburg, 1971; Lachenbruch and Sass, 1973, 1980). Taken together, the Cajon Pass in situ stress and heat flow measurements (Lachenbruch and Sass, this issue) support a conceptual model of the San Andreas system in which the San Andreas is extremely weak with respect to the surrounding crust.

INTRODUCTION

A long-standing problem in understanding the mechanics of earthquakes is the level of shear stress acting on major crustal faults like the San Andreas fault. Application of Mohr-Coulomb faulting theory and laboratory-derived coefficients of friction in the range of 0.6–1.0 [e.g., *Byerlee*, 1978] imply average levels of shear stress for the seismogenic part of the fault (the upper ~15 km) that are about a factor of 5 higher than stress levels inferred from numerous heat flow measurements which indicate a complete absence of frictionally generated heat on the fault [*Brune et al.*, 1969; *Henyey and Wasserburg*, 1971; *Lachenbruch and Sass*, 1973, 1980, 1988, this issue]. This discrepancy is sometimes referred to as the San Andreas stress/heat flow paradox.

The importance of resolution of this paradox is multifold. Are laboratory-derived friction data and experimentally based earthquake instability mechanisms such as stick-slip and time-dependent friction that are associated with high friction levels relevant to earthquakes along major faults like the San Andreas [e.g., *Brace and Byerlee*, 1966; *Byerlee*, 1970; *Dieterich*, 1979]? Are conceptual models of the state of stress in the lithosphere in which the overall average stress levels are defined by the "high" frictional strength of the upper crust and upper mantle relevant to plate boundaries [e.g., *Sibson*, 1982, 1983; *Kirby*, 1980; *Chen and Molnar*, 1983; *Smith and Bruhn*, 1984; *Molnar*, 1988]? What are the relative magnitudes of the forces that drive and resist plate motion along plate boundary [e.g., *Lachenbruch and Sass*, 1973, 1980, this issue; *Hanks*, 1977]? Do earthquake stress drops (typically in the range of ~1–10 MPa [*Kanamori and Anderson*, 1975]) represent near-complete relief of shear stress along the plate boundary or only a relatively minor perturbations superimposed on an ambiently high level of shear [e.g., *Lachenbruch and Sass*, this issue; *Shamir and Zoback*, this issue]?

The implications of these questions are obviously far reaching. Yet despite the fact that discussions of the possible weakness of the major transform faults like the San Andreas have been going on for over two decades (see also *Lachenbruch and Thompson* [1972] and *Oldenburg and Brune* [1972, 1975] for arguments that motion along oceanic transforms is also resisted by extremely little shear stress), little attention has been paid to the implications of the weak fault hypothesis. One reason for this is that heat flow measurements are

Paper number 91JB02175.
0148-0227/92/91JB-02175$05.00

an indirect method for measuring average stress. Also, as nearly all the available conductive heat flow data near the San Andreas have come from holes only about 300 m deep, it has been proposed that broad-scale convective heat transport or some other process makes inferences about stress levels from heat flow measurements questionable [*O'Neil and Hanks*, 1980]. Another problem with simply assuming that major faults are extremely weak is that in situ stress measurements indicate differential stress levels consistent Mohr-Coulomb theory and laboratory-derived coefficients of friction in the range of 0.6–1.0 in studies conducted in a wide variety of tectonic environments around the world [e.g., *Raleigh et al.*, 1972; *McGarr and Gay*, 1978; *Brace and Kohlstedt*, 1980; *Zoback and Hickman*, 1982; *Pine et al.*, 1983; *Zoback and Healy*, 1984; *Stock et al.*, 1985; *Baumgärtner and Zoback*, 1989; *Baumgärtner et al.*, 1990]. Why should the San Andreas be so different, especially as laboratory experiments on fault gouges obtained at the surface or very shallow depth indicate relatively high coefficients of fraction generally consistent with those for intact rock [e.g., *Morrow et al.*, 1982]?

The Cajon Pass Scientific Drilling Project was designed to address the questions of stress and heat flow at depth along the San Andreas. Would the implications of the shallow heat flow data be confirmed by data obtained from greater depth? Would stress magnitudes at depth be consistent with applicability of Mohr-Coulomb theory and laboratory-derived coefficients of fraction of about 0.6–1.0 and essentially hydrostatic pore pressure (following *Brace and Kohlstedt* [1980], we shall refer to this as "Byerlee's law") or be found to be consistent with the much lower values suggested by the heat flow data? These questions could only be addressed by drilling near the San Andreas to measure heat flow at depths greater than the influence of possible thermal convection [e.g., *Lachenbruch and Sass*, 1988, this issue] and to measure stress at depths at which stress magnitudes (consistent with Byerlee's law) would substantially exceed the maximum stress levels implied by the heat flow data. An overview of the Cajon Pass project was presented by *Zoback et al.* [1988*b*] in a special issue of *Geophysical Research Letters* that contained 36 papers reporting preliminary results of the first phase of the project after drilling had reached a depth of 2.1 km. The papers in this special section of the *Journal of Geophysical Research* summarize results obtained to a depth of 3.5 km. Technical and operational aspects of the Cajon Pass drilling project are discussed by *Wicklund et al.* [1988, 1990].

Since the initiation of the Cajon Pass project in 1986, additional arguments have been made about the frictional strength of the San Andreas fault based upon the orientation of maximum principal stress in a relatively broad zone ($\sim\pm100$ km) on either side of the fault. Abundant data in Central California show that the direction of maximum horizontal compression is almost perpendicular to the strike of the San Andreas [*Zoback et al.*, 1987; *Mount and Suppe*, 1987; *Oppenheimer et al.*, 1988; *Wong*, 1990], indicating that there is extremely little resolved shear stress on the fault. *Solomon et al.* [1989] and *Wilcock et al.* [1990] have recently reported a similar finding for oceanic transforms using well-constrained (off-transform) earthquake focal plane mechanisms. These data further define the manner in which the stress measurement in the Cajon Pass borehole can test and illuminate the hypothesis that the San Andreas is quite weak. For example, one important question raised by the stress orientation data is whether the entire crust along plate boundaries has low strength or whether there is a marked contrast in strength between the crust adjacent to the fault and the fault itself. The latter case was proposed by *Kanamori* [1980] on the basis of the large difference between the ~100 MPa strength of the crust implied by Byerlee's law and the universally low observations of earthquake stress drops determined from both geodetic and seismologic measurements (~1–10 MPa [*Kanamori and Anderson*, 1975]). *Zoback et al.* [1987] and *Mount and Suppe* [1987] proposed similar models in an attempt to explain the origin of the fault normal compression observed along the San Andreas of central California. By measuring stress magnitudes and the orientation of principal stresses in the Cajon Pass well, we can directly test this "strong crust/weak transform" hypothesis by contrasting the level of shear stress resolved on the San Andreas with the absolute levels of shear stress in the crust.

Another important aspect of the Cajon Pass stress measurements with respect to the implications of stress orientation data from central California is that no clear pattern of fault normal compression is seen in southern California [see *Zoback et al.*, 1987; *Jones*, 1988; *Hauksson*, 1990; *Shamir and Zoback*, this issue], and it is not clear if the arguments based on stress orientation data from north of the big bend (i.e., north of Fort Tejon) apply to the southernmost San Andreas. On the basis of focal plane mechanisms from earthquake near the San Andreas, *Jones* [1988] has argued that the direction of maximum horizontal compression is at a higher angle to the southern San Andreas than predicted by conventional faulting theory (~65° rather than 30°–45°). While these results imply that the San Andreas has low frictional strength, she suggests that the southern San Andreas may not be "as weak" as the central San Andreas because the directions of maximum horizontal stress implied by the earthquake focal plane mechanisms are not nearly orthogonal to the fault (as is in central California). Could there, in fact, be marked differences in strength along various sections of the San Andreas? While this may be true, it is important to note that the evidence for near fault normal compression in central California comes both from regions where the San Andreas produced major earthquakes in 1906 and 1857 and where it is currently creeping [see *Zoback et al.*, 1987, Figure 1]. It is also important to note that there is a fundamental difference between the use of earthquake focal plane mechanisms to infer stress orientation in the studies of *Jones* [1988] and of *Zoback et al.* [1987]. In the former case, only earthquakes within ±10 km of the San Andreas fault were used to assess stress orientation. In the latter case, only earthquakes were used that were clearly not on the San Andreas fault (or its principal branches) to avoid the potentially large difference (as much as 90°) between P axes and $S_{H\max}$ directions in cases when slip is occurring on a low friction fault [*MacKenzie*, 1969].

The location of the Cajon Pass borehole is shown in Figure 1*a* on a map of active faults along a section of the San Andreas fault in southern California that was derived from mapping by *Weldon* [1986] and *Matti et al.* [1985]. The drill site is only 4 km from the San Andreas, in an area of moderate topography, and along a section of the fault which is apparently quite late in the seismic cycle. The best available evidence indicates that the last major strike-slip

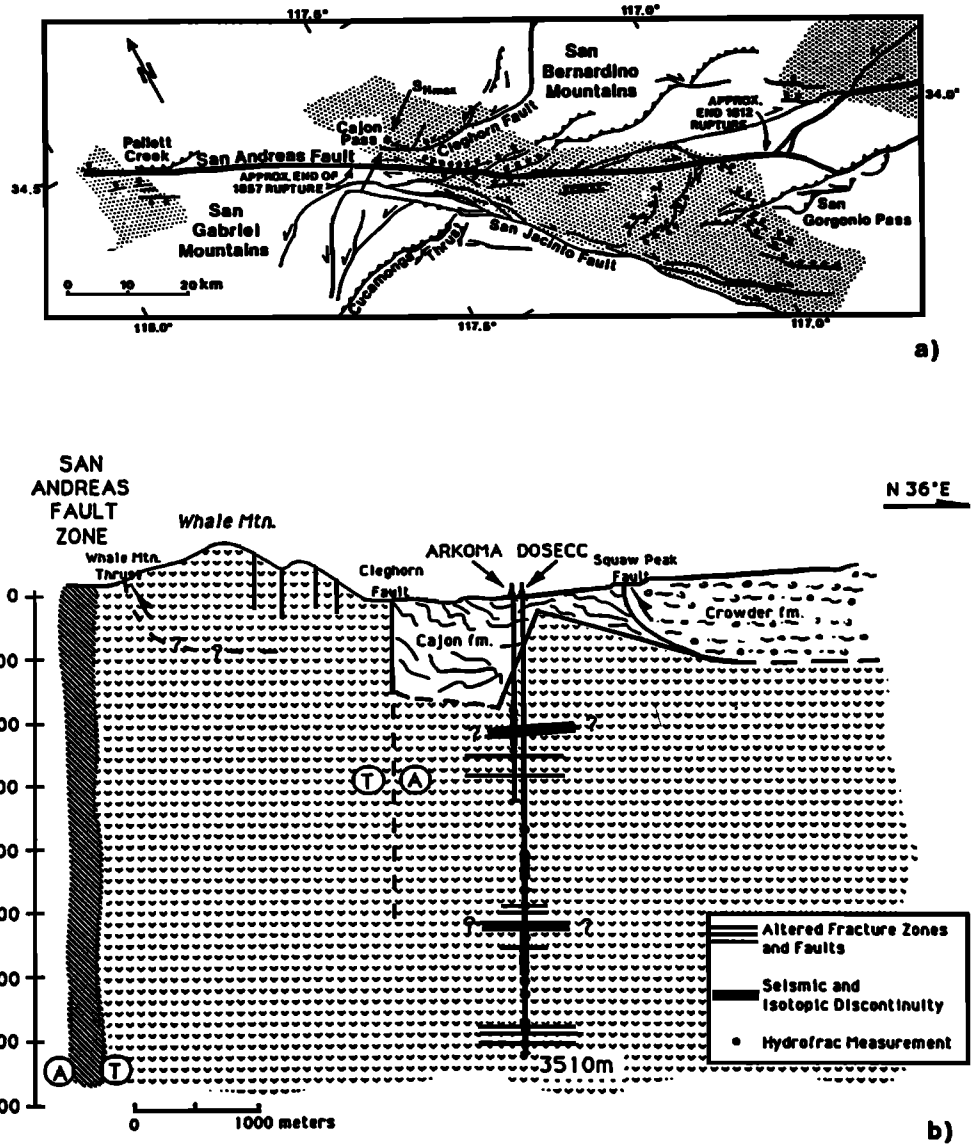

Fig. 1. (*a*) Map of active faults along the southern San Andreas and San Jacinto fault systems in southern California derived from Figure 1 of *Weldon and Springer* [1988] (after mapping by *Weldon* [1986] and *Matti et al.* [1985]). The direction of lateral motion is shown on faults with known strike-slip motion, barbs are shown on the hanging wall side of faults with reverse motion, and the bar and ball symbol is shown on the footwall side of faults with normal displacement. The stippled areas indicate regions in which the style of secondary faulting is extensional. Areas where the style of secondary faulting is compressional are unshaded. The location of the Cajon Pass borehole is shown with the average direction of maximum horizontal compression of N57°E [*Shamir and Zoback*, this issue]. Other locations of note along the San Andreas are the southeastern ends of rupture in the major earthquakes of 1812 and 1857 (after *Sieh* [1978] and *Jacoby et al.* [1988], respectively). In both cases, the earthquakes ruptured far to the northwest along the San Andreas. (*b*) Generalized geologic cross section perpendicular to the San Andreas fault through the sites of the Arkoma and DOSECC boreholes at Cajon Pass (after L. T. Silver and E. W. James, written communication, 1991). With the exception of the ~50-m surface spacing between the boreholes that is exaggerated for clarity, the schematic cross section is at approximately true scale. No differentiation of basement rocks is shown, although the depths of major seismic and isotopic discontinuities are shown, as well as other zones of unusually dense faulting. The depths at which hydrofrac measurements were made in the two wells is shown. T and A denote toward and away for strike-slip faults. Note that the sense of motion on the Cleghorn fault is left-lateral, opposite that of the San Andreas [*Meisling and Weldon*, 1982; *Weldon*, 1986; R. J. Weldon et al., unpublished report, 1981]. Neither the Whale Mountain or Squaw Peak faults are currently active. The high-angle fault between the two wells [see *Silver and James*, 1988*a*] was unknown prior to drilling the holes.

earthquake at this site occurred in 1812, when a 4.5-m right-lateral offset occurred at nearby Cajon Creek [*Weldon*, 1986; *Sieh et al.*, 1989; *Jacoby et al.*, 1988]. Based on a long-term slip rate of about 25 mm/yr at Cajon Pass [*Weldon and Sieh*, 1985; *Weldon*, 1986], approximately 4.4 m of potential slip has accumulated since 1812. Thus the level of shear stress at this site should be about equal to its value at the time of the 1812 event.

Detailed geology of the Cajon Pass site is described by *Weldon* [1986], *Meisling and Weldon* [1989], *Silver and*

James [1988*a*], and *Ehlig* [1988*a*, *b*]. Note in Figure 1*a* that the Cajon Pass drill site is within one of several extensive regions along the San Andreas and San Jacinto faults where the style of active secondary faulting is extensional (the stippled areas in Figure 1*a* are taken from Figure 1 of *Weldon and Springer* [1988]). The Cleghorn fault, which strikes subparallel to the San Andreas in the vicinity of the drill site, is also of important note. R. J. Weldon et al. (Neotectonics of the Silverwood Lake area, San Bernadino County, unpublished report to California Department of Water resources to accompany 50-sq. mile map of the San Bernadino Mountains around the Silverwood Lake Reservoir, 1981), *Meisling and Weldon* [1982], and *Weldon* [1986] discuss evidence for left-lateral strike-slip and normal fault displacements on the Cleghorn in Quaternary time.

A schematic geological cross section through the Cajon Pass site is shown in Figure 1*b* (modified after L. T. Silver and E. James (written communication, 1991). The Whale Mountain and Squaw Peak thrusts shown in Figure 1*b* are no longer active. Zones of particularly intense faulting and zones which are distinct seismic and isotopic discontinuites (simplified after L. T. Silver and E. W. James (written communication, 1991)) are shown in Figure 1*b*. Two relatively deep boreholes exist at the Cajon Pass site, an abandoned wildcat well drilled at the site by Arkoma Production Company and the scientific research borehole drilled by the university consortium Deep Observation and Sampling of the Continental Crust (DOSECC) in conjunction with the U.S. Geological Survey and Department of Energy. Drilling of the DOSECC hole only ~50 m from the Arkoma hole revealed a previously unknown high-angle fault that cuts between the two wells [see *Silver and James*, 1988*b*].

Fractures and faults were found throughout the borehole. A discussion of macroscopic and microscopic fractures and associated chemical alteration that can be observed in core samples and thin section analysis is presented by *Silver and James* [1988*a*, also submitted manuscript, 1990], *Vernik and Nur* [this issue], and *Morrow and Byerlee* [1988, this issue]. *Vincent and Ehlig* [1988] describe fractures and associated hydrothermal alteration in basement rocks exposed in the region surrounding the drill site. Detailed studies of fractures detected through geophysical logging (principally with the ultrasonic borehole televiewer and formation microscanner) are discussed by *Barton and Moos* [1988] and *Barton and Zoback* [this issue] in the crystalline rocks in the lower part of the hole. *Pezard et al.* [1988] discuss fractures and other structures identified through logging in the sedimentary section of the upper part of the hole. Stress-induced well bore breakouts were ubiquitous in the lower half of the borehole. These are described and discussed in detail by *Shamir and Zoback* [this issue]. *Vernik and Zoback* [1989, 1990] describe a comprehensive series of strength tests specifically aimed at determining whether rock strength anisotropy induced by foliation had any appreciable affect on the occurrence of the stress-induced well bore breakouts. They concluded that azimuthal strength variations around the borehole had very little effect on the generation of well bore breakouts as (1) the foliation in the borehole was almost everywhere subhorizontal (dipping less than 45°; see also *Silver and James* [1988*a*]) and (2) only one rock type showed appreciable rock strength anisotropy (biotite-rich amphibolites and schists) which comprised less than 5% of the lithologic column (see also, *Vernik and Zoback* [this issue]). The same conclusion was reached by *Shamir* [1990] and *Shamir and Zoback* [this issue] as no correlation between breakout orientations and lithology was found.

In situ stress measurements were made at the Cajon Press site in three stages. *Healy and Zoback* [1988] presented a preliminary interpretation of hydraulic fracturing stress measurements made at depths of 0.9 and 1.3 km depth in the Arkoma well (stage I) and between 1.86 and 2.1 km depth in the Cajon Pass borehole drilled by DOSECC (stage II). In this paper we present hydraulic fracturing stress measurements to 3.5 km depth in addition to measurements of stress orientation and estimates of $S_{H\max}$ magnitude obtained from analysis of well bore breakouts (see also *Shamir and Zoback* [this issue] and *Vernik and Zoback* [this issue]). As discussed by *Healy and Zoback* [1988], the stress state observed in the upper 2.1 km at the Cajon Pass site is consistent with the style of active faulting around the drillsite (see also *Weldon and Springer* [1988]). However, the orientation of maximum horizontal stress in the upper 2.1 km resulted in a component of left-lateral shear on planes parallel to the San Andreas which suggests that either the site was decoupled from that of the San Andreas fault or that the San Andreas was extremely weak. In this paper we follow up these observations and hypotheses and discuss the implications of the state of stress measured in the Cajon Pass borehole for the frictional strength of the San Andreas and adjacent crust.

OVERVIEW OF IN SITU STRESS MEASUREMENTS

Measurements of in situ stress magnitude and orientation were made at the Cajon Pass drill site using the hydraulic fracturing stress measurement technique [e.g., *Haimson and Fairhurst*, 1967, 1970] and detailed observations of stress-induced well bore breakouts [e.g., *Bell and Gough*, 1979, 1983; *Gough and Bell*, 1981; *Cox*, 1983; *Zoback et al.*, 1985]. As presented in detail below, the hydraulic fracturing data provided 23 measurements of the least horizontal principal stress, $S_{h\min}$, as function of depth, six estimates of the maximum horizontal stress, $S_{H\max}$, and four measurements of the direction of maximum horizontal compression (Table 1) were also obtained from the hydraulic fracturing tests. As discussed below, 12 additional estimates of $S_{H\max}$ were obtained through detailed analysis of well bore breakouts.

Hydraulic fracturing. Since it was first described as a stress measurement method by *Haimson and Fairhurst* [1967], the hydraulic fracturing technique has become widely used for measurement of in situ stress magnitude and orientation in boreholes. Three compilations of papers [*Zoback and Haimson*, 1983; *Stephansson*, 1986; Haimson, 1989] provide useful summaries of worldwide experience with hydraulic fracturing (hydrotrac) as an in situ stress measurement method. Among the strengths of the hydrofrac method is its ability to determine accurately the magnitude of least principal stress. As hydraulic fractures propagate away from a borehole in a manner to minimize the energy required for propagation, they propagate in a plane perpendicular to the least principal stress, essentially independent of material properties and conditions immediately adjacent to the borehole [cf. *Hubbert and Willis*, 1957; *Warren and Smith*, 1985]. It is widely recognized that when used for stress measurements in crystalline rock, straightforward interpretation of hydraulic fracturing pressure data yields reliable information

TABLE 1. In Situ Stress Measurements

Depth,* m	Hydraulic Fracturing			Remarks	Well Bore Breakouts	
	S_{hmin}, MPa	S_{Hmax}, MPa	Strike/Dip S_{Hmax}		S_{Hmax}, Azimuth†	S_{Hmax},‡ MPa
907	12.9 ± 0.9			preexisting fractures		
918	12.1 ± 0.2	19.1 ± 7.6		hydrofracture		
928	13.6 ± 0.4	27.8 ± 8.2		hydrofracture		
938	14.0 ± 0.3			preexisting fractures		
991	13.7 ± 0.5			preexisting fractures		
1044	15.6 ± 0.3			preexisting fractures		
1178	19.1 ± 1.7			preexisting fractures		
1187	19.8 ± 0.5			preexisting fractures		
1277	20.6 ± 0.3	19.1 ± 7.9?		hydrofrac, anomalous high T?		
1852					035 ± 11	68 ± 8
1862	>36.1			preexisting fractures	089 ± 7	
2048	39.9 ± 0.2	79.3 ± 7.6	096/80	hydrofracture	092 ± 25	
2052	45.0 ± 0.2		090/87	hydrofracture	092 ± 25	
2085	48.4 ± 0.5		084/85	hydrofrac/packer problem	075 ± 20	
2091	47.9 ± 0.4		092/81	hydrofracture	085 ± 15	
2095					96 ± 11	77 ± 14
2163	32.3 ± 0.2			preexisting fractures	92 ± 14	
2188	30.2 ± 0.3			preexisting fractures	no BOs	
2375	34.3 ± 0.2			preexisting fractures	variable	
2438					092 ± 8	78 ± 12
2500					no BOs	<73
2652	34.9 ± 0.2	66.8 ± 7.6		hydrofracture	variable	
2661	32.9 ± 0.2	70.0 ± 7.6		hydrofracture	no BOs	
2670	37.1 ± 0.3			preexisting fractures	no BOs	
2685	41.0 ± 0.2			preexisting fractures	variable	
2705					071 ± 8	85 ± 13
2803					071 ± 8	93 ± 27
2805					071 ± 8	105 ± 17
2857	~40.9			hydrofracture/packer problem	113 ± 7	
2974					123 ± 14	114 ± 17
2980					060 ± 14	99 ± 25
3122					no BOs	<85
3398					127 ± 21	108 ± 33
3486	82.9 ± 0.3			preexisting fractures/single packer	57 ± 21	
3507						123 ± 21

BO, breakouts.

*The stress measurements at depths between 907 and 1277 m were made in the Arkoma well at the Cajon Pass site [See *Healy and Zoback*, 1988]; all deeper measurements were made in the DOSECC hole.

†See *Shamir and Zoback* [this issue]; average breakout orientations for depths close to those of the hydrofracs are shown.

‡See *Vernik and Zoback* [this issue]; depth corresponds to average depth from which sample strengths with measured.

on the magnitude of the least principal stress. As discussed at length below, the most significant problem with using the hydraulic fracturing for in situ stress measurements is determination of the maximum horizontal compressive stress S_{Hmax}.

While we basically utilized a conventional "open-hole" inflatable straddle-packer system to conduct the hydrofrac tests, we made a number of modifications of standardly used equipment for use in these experiments. Noteworthy developments included (1) improved inflatable high-pressure straddle packers for the relatively large diameter of the DOSECC borehole, (2) a downhole pressure gauge carrier system that made it possible to measure simultaneously pressure in the hydrofrac interval, within the inflatable packer elements, and below the straddle-packer assembly, and (3) a sophisticated monitoring system that simultaneously recorded pressure and flow from redundant instruments on two independent computer systems at the surface. The first development was necessary because high-pressure inflatable packers were previously not commercially available. The development of the downhole gauge carrier enabled us to analyze tests more fully in which unusual pressure-time records were obtained and enabled us to test for packer leaks or flow past the lower packer. The third development insured the highest possible data accuracy (six different pressure gauge systems were used, including redundant high-precision quartz pressure transducers) so that the validity of any given test would not be compromised by failure or calibration problems with any given instrument. No significant difference between surface pressure and interval pressure was detected once a correction for the hydrostatic head was made. Utilization of this system also meant that tests could proceed as planned even if a given monitoring instrument or one of the recording systems failed as the test was proceeding. Taking into account both the difficult conditions encountered in relatively deep holes and the great expense associated with rig time, the purpose of these modifications helped to improve the accuracy of each measurement as well as the probability that any given test would be successful. Despite these developments and other precautions, the combination of poor hole conditions and packer problems made a number of the attempted hydrofrac tests unsuccessful. Thus, while appreciable progress was made in packer development, further improvements in

packer systems for future deep hydrofrac tests are clearly necessary. *Healy and Zoback* [1988] describe a number of the experimental techniques in more detail.

The distribution of the hydrofrac measurements as a function of depth in the two holes is shown in Figure 1*b*. As shown, all of the stress measurements were made in crystalline basement rocks. The fractures and faults that were encountered throughout the hole often made identification of suitable intervals for hydraulic fracturing difficult. Stress-induced well bore breakouts were also widespread in the hole at depths below 1.75 km [*Shamir and Zoback*, this issue] and further limited the possibility to conduct the hydraulic fracturing tests. Fortunately, stress-induced breakouts have proven to be an extremely reliable method for determining in situ stress orientations [*Bell and Gough*, 1979, 1983; *Zoback and Zoback*, 1980, 1989; *Blümling et al.*, 1983; *Plumb and Cox*, 1987; *Zoback et al.*, 1987; *Mount and Suppe*, 1987; *Zoback et al.*, 1989] and provide a wealth of important data about the stress field encountered in the Cajon Pass borehole.

For the case of a vertical well drilled into isotropic rock and one principal stress acting parallel to the borehole, Figure 2*a* illustrates the theoretical relationship between the positions around the borehole where hydraulic fractures and well bore breakouts occur. Hydraulic fractures will initiate in a vertical plane at the azimuth of maximum horizontal principal stress $S_{H\max}$ in response to pressurization of the borehole (ΔP_b) to the pressure at which the stress concentration around the well bore reaches the tensile strength of the rock, T, at the azimuth of $S_{H\max}$. The orientation of hydraulic fractures has been found to be a reliable indicator of the direction of maximum horizontal compression in many studies (see also stress complications of *Haimson* [1977], *Zoback and Zoback* [1980, 1988], and *Zoback et al.* [1989]). Numerous studies in which earthquake focal plane mechanisms have been used to indicate the direction of principal stresses show, with some rare exceptions, that one principal stress is essentially vertical [*Zoback and Zoback*, 1980, 1988; *Zoback et al.*, 1989]. Of particular note to this study is a similar finding by *Jones* [1988], who inverted earthquake focal mechanism data to determine stress tensors within ±10 km of the southern San Andreas. A number of in situ stress measurements have also shown that one principal stress is usually very close to vertical [e.g., *Haimson*, 1976; *McGarr and Gay*, 1978; *Zoback and Hickman*, 1982; *Evans and Engelder*, 1989; *Baumgärtner and Zoback*, 1989]. Modelling of topographically induced stresses at the Cajon Pass drill site also indicates that no appreciable deviation from a vertical principal stress is induced by regional topography [*Liu and Zoback*, this issue]. We therefore assume that one principal stress is approximately vertical in the analysis of the hydrofrac and breakout data at the Cajon Pass site.

Well bore breakouts. Stress-induced well bore breakouts form over some range of angles at the azimuth of least horizontal principal stress, $S_{h\min}$, if the naturally occurring compressive stress concentration exceeds the compressive strength of the rock, C [see *Bell and Gough*, 1979; *Zoback et al.*, 1985; *Moos and Zoback*, 1990]. The ultrasonic borehole televiewer [*Zemanek et al.*, 1970] produces data that can be used to recreate the precise shape of the hole with a resolution that is ~1 cm vertically and ~1 mm radially, when the data quality is good. Figure 2*b* shows a perspective view of a section of the Cajon Pass borehole at 2088 m constructed by special processing of borehole televiewer data [*Barton*, 1988; *Barton et al.*, 1991]. As can be seen in the image, the induced hydraulic fracture and naturally occurring well bore breakout are orthogonal to one another as expected by theory. Similar results have also been found in a number of other studies [*Hickman et al.*, 1985; *Stock et al.*, 1985; *Paillet and Kim, 1985; Plumb and Cox*, 1987; *Baumgärtner et al.*, 1990]. The most common method used to determine hydraulic fracture orientation involves use of magnetically oriented impression packers which are pressed against the borehole wall after a hydraulic fracture is made [e.g., *Anderson and Stahl*, 1967]. While this technique is used frequently in relatively shallow holes, it is extremely time consuming, and thus expensive, to determine the orientation of hydraulic fractures in relatively deep holes. Also, it can often produce poor results in deep wells because of damage to the impression packer that occurs when it is being lowered and raised in the well. For these reasons, we only attempted to make several hydrofrac orientations at about the middepth of the hole for comparison with the breakout observations (Table 1). As illustrated in Figure 2*c*, at a depth of 2052 m, use of an impression packer also shows that the hydrofracs and breakouts are orthogonal to one another. The sinusoidal trace of the hydrofrac (straight-line segments) on the impression packer indicates a strike of 90° and dip of ~87°. As the comparison between stress orientations determined with hydraulic fracturing and breakouts was so good in both the Cajon Pass borehole and other scientific boreholes worldwide, we decided to rely primarily on the breakouts for in situ stress orientation in the Cajon Pass experiment. *Shamir and Zoback* [this issue] report a detailed analysis of breakouts in the Cajon Pass borehole. This study yielded approximately 32,000 observations of the orientation of well bore breakouts (and thus the least horizontal principal stress orientation) over a depth range of 1.7–3.5 km.

As mentioned above, detailed analysis of the shapes of well bore breakouts was also used to supplement the information on the magnitude of $S_{H\max}$ available from hydraulic fracturing. This technique basically involves independent knowledge of $S_{h\min}$ from hydraulic fracturing and strength of the rock [*Barton et al.*, 1988; *Moos and Zoback*, 1990]. In laboratory tests, *Herrick and Haimson* [1990] have recently documented an increase of breakout size with increasing stress. *Vernik and Zoback* [this issue] further developed the technique used by *Barton et al.* [1988] for estimation of $S_{H\max}$ to improve the accuracy of such in situ stress estimations [e.g., *Maloney and Kaiser*, 1989]. *Vernik and Zoback* [this issue] made detailed rock strength measurements and utilized a generalized failure criterion for the formation of breakouts based on the effective strain energy concepts of *Weibols and Cook* [1968]. Combination of the breakout observations with the detailed $S_{h\min}$ values provided by the hydraulic fracturing tests and the rock strength measurements allowed them to make a profile of $S_{H\max}$ estimates in the Cajon Pass well. Together, utilization of the hydraulic fracturing and well bore breakout techniques resulted in a fairly complete profile of both stress magnitude and orientation from 0.9 to 3.5 km at the Cajon Pass site.

RESULTS

Least principal stress. While it is relatively straightforward to determine the magnitude of the least principal stress

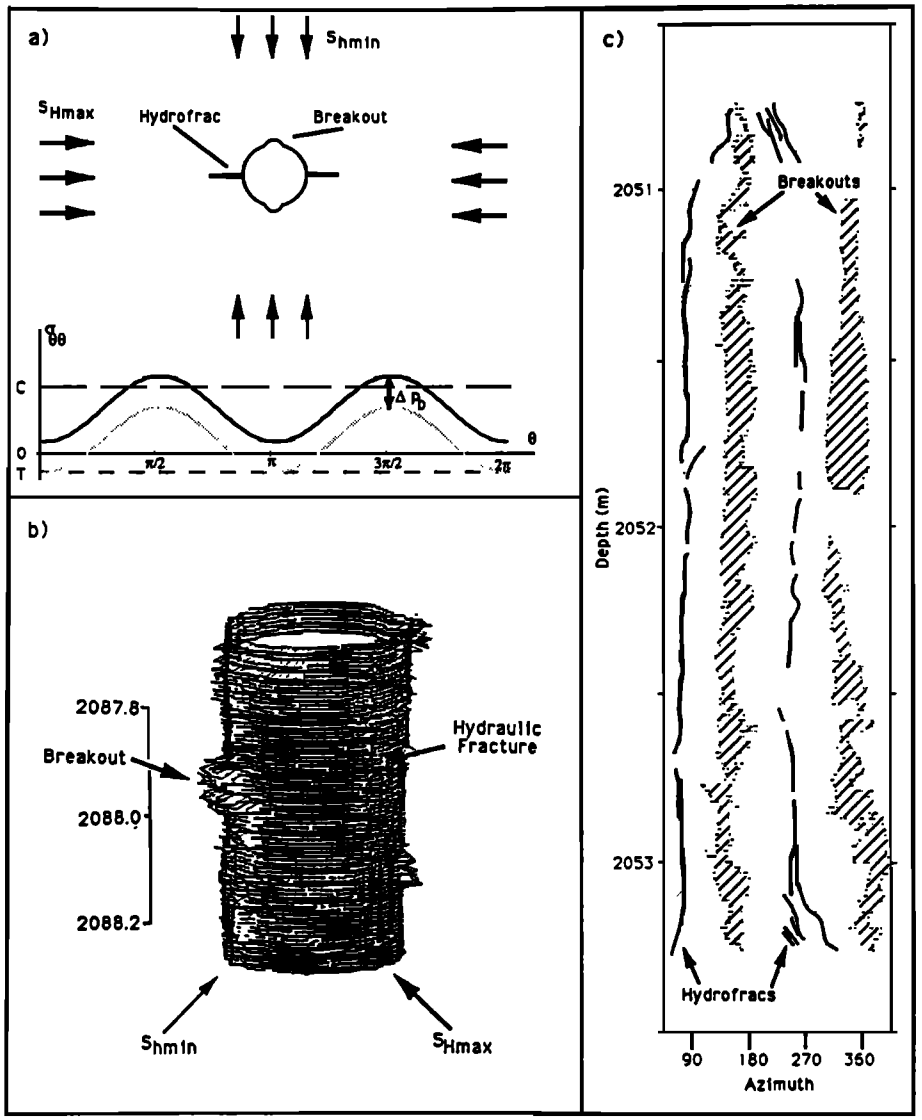

Fig. 2. (*a*) Schematic diagram of the relationship between the location of hydraulic fractures and stress-induced well bore breakouts in a vertical wellbore. A schematic variation of the circumferential stress (σ_{qq}) around the well bore is also shown based on the equations of *Kirsch* [1898]. Breakouts are expected when the concentration of hoop stress (maximum at the azimuth of the least horizontal principal stress, S_{hmin}) exceeds the compressive strength of the rock. Hydraulic fractures occur at the azimuth of S_{Hmax} in response to a tensile circumferential stress induced by the combined effects of the stress concentration and pressurization of the well bore that exceeds the tensile strength of the rock. (*b*) Perspective view of a section of the borehole at around 2088 m where a hydraulic fracture was induced and a small well bore breakout was present. The image was produced from ultrasonic borehole televiewer data that has a radial precision of about 1 mm. The diameter of the borehole is 15 cm. The breakout and hydrofrac are orthogonal as expected by theory. (*c*) Tracing of an impression packer from a depth of 2052 m that also shows the orthogonal relationship between an induced hydraulic fracture and naturally occurring wellbore breakouts. The thin lines representing the hydrofrac correspond to distinct, narrow (<1 mm) ridges on the impression packer. They define a steep sinusoidal trace with a strike of 90° and dip of 87°. The location of well bore breakouts were indicated by broad, raised areas on the impression packer with small imbedded rock fragments.

using the hydraulic fracturing technique, the accuracy of hydrofrac measurements depends strongly on the correct interpretation of the pressure-time records obtained during the experiment. Several standard data interpretation methods were used in this study for determination of the least principal stress. These methods involve using the pressure-time data to determine the instantaneous shut-in pressure (ISIP) and low-flow-rate pumping pressures and are widely described in hydraulic fracturing literature. To improve the interpretation of the pressure-time data, however, several new interactive data interpretation methodologies were also used that have been described in detail by *Baumgärtner and Zoback* [1989]. Utilization of these techniques made it possible to track small changes of pressure, flow rate, and pressurization rate as a function of time and thus determine the least principal stress from the pressure data with several independent methods. While the results obtained with the different methods varied very little, as shown by the estimates of uncertainty in Table 1, these techniques were employed to yield redundant measures of the least principal

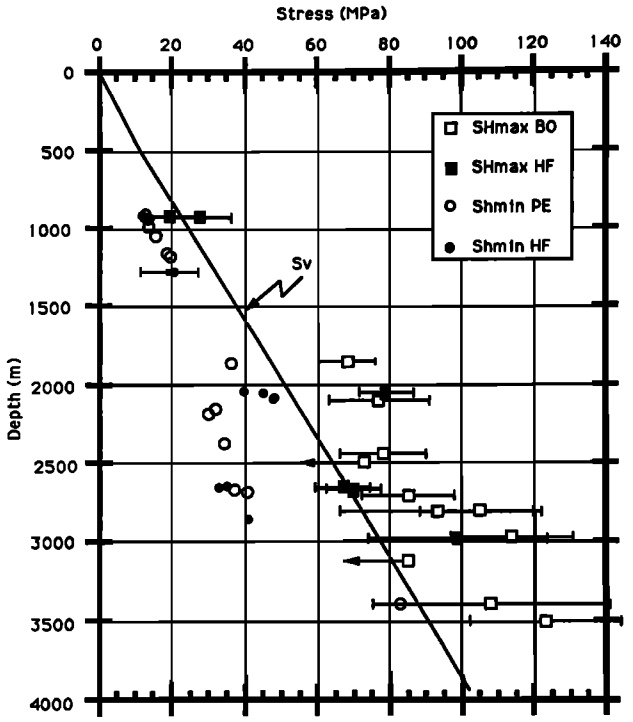

Fig. 3. Magnitude of least principal horizontal stress, S_{hmin}, and estimates of maximum horizontal principal stress, S_{Hmax}, as a function of depth at the Cajon Pass site. The measurements at depths shallower than 1277 m were made in the Arkoma borehole and the deeper measurements were made in the DOSECC borehole. The terms BO, HF, and PE refer to the S_{Hmax} estimates determined from the breakout analysis of *Vernik and Zoback* [this issue], the S_{hmin} and S_{Hmax} values determined from the hydrofrac tests, and the S_{hmin} values determined from the hydrofrac tests in zones with pre-existing fractures, respectively. The line labelled S_v is the estimated value of the vertical stress based on the average density of the rocks. The manner in which the hydrofrac S_{Hmax} were computed considers intergranular pore pressure to have no effect on the breakdown pressure. This assumption tends to make the values shown upper bound estimates.

stress for each test and to provide as a good an estimate as possible of the range of uncertainty of each stress measurement.

Two types of hydrofrac measurements were made. The tests indicated by the word "hydrofrac" in Table 1 and Figure 3 refer to relatively conventional, open-hole hydraulic fracturing tests in the best intervals of rock that could be found in the hole (i.e., intervals where no breakouts or preexisting fractures were present and where the rock type was relatively uniform). The other type of test (referred to with the term "preexisting fractures") involved pressurization of a zone where there were known preexisting natural fractures as indicated by borehole televiewer logging. In the Arkoma borehole (the stress measurements in Table 1 and Figure 3 that were made to a depth of 1277 m), this was done repeatedly to lower the breakdown (fracture initiation) pressure. High viscosity drilling mud had been left in the Arkoma borehole for approximately 2 years prior to the stress measurements and had resulted in anomalously high apparent tensile strengths for a number of the tests [see *Healy and Zoback*, 1988]. In the DOSECC borehole, this type of test was also performed to reduce the maximum pumping pressures in about half the tests. While it is impossible to determine the magnitude of S_{Hmax} from the tests in the zones with preexisting fractures, the six preexisting fracture tests and three conventional hydraulic fracturing tests yielded nearly identical values for S_{hmin} in the tests conducted in the Arkoma hole (907–1277 m) and the same was found to be true at 2650–2857 m in the DOSECC borehole. The four values of the least principal stress that are anomalously high around 2050 are all conventional hydrofracs. The tests are discussed in more detail below.

Figure 3 indicates that at nearly all depths in the hole S_{hmin} is substantially lower than the vertical principal stress, S_v, as estimated from the density of the rocks. One of the most striking things about the variation of S_{hmin} with depth, however, is the localized increase of S_{hmin} at about 2100 m. The measurements at 2085 and 2091 m indicate that the magnitude of S_{hmin} is almost equal to that of the overburden, S_v, whereas the deeper and shallower measurements show that it is considerably less.

Figure 4 is an example of the pressure and flow data that were recorded at the surface that also indicates the abruptness of the change of magnitude of the least principal stress at about 2100 m. Figures 4*a* and 4*b* show the last three pressurization cycles from the test at 2091 m, and Figure 4*c* shows the five pressurization cycles of the test at 2375 m. Corresponding to each pressure record is a measure of the flow rate into the hydrofrac test interval during pumping (the top panel in each figure) and periods when the pressurization system was opened and flow was allowed to "flow back" out of the fracture (the shaded bars in the middle panel). The pressure buildups seen after the second and third pressurization cycles shown for the test at 2091 m (Figures 4*a* and 4*b*) shows that when the flow back is abruptly terminated due to closing a surface valve, a pressure buildup occurs due to continued flow out of the fracture as the pressure in the fracture is greater than that in the wellbore.

In Figure 4*a*, the last two pumping cycles from the test at 2091 m clearly indicate a shut-in pressure and low-flow-rate pumping pressure that stabilize at a value of about 25 MPa [see *Hickman and Zoback*, 1983]. When the precise value of the hydrostatic head is added, the value determined for S_{hmin} for this test was 47.9 ± 0.4 MPa (Table 1). The last pressurization cycles for the test at a depth of 2375 m (Figure 4*c*) shows that the low flow rate pumping pressure and shut-in pressure is only about 10 MPa, less than half the measured surface pressure for the test shown in Figures 4*a* and 4*b*. After adding the hydrostat, the best determined value for S_{hmin} at 2375 m is 34.3 ± 0.2 MPa. It is clear, therefore, that the abrupt change in S_{hmin} indicated by the tests at about 2100 m is associated with rather large changes in pumping and shut-in pressures. The deepest stress measurement at about 3.49 km, involved setting a single packer at the bottom of casing and pressurizing the open-hole section of the borehole below the casing. This data point also indicates that the least principal stress is almost equal to the weight of the overburden. Unfortunately, there are insufficient data to define the nature of the change of stress between this point and that at 2857 m. A possible cause for the two zones of anomalously high values of S_{hmin} observed in the borehole is presented in the Discussion section below.

Maximum horizontal principal stress. The basic mechanics of initiation of hydraulic fractures was first worked out for a porous, impermeable material by *Hubbert and Willis* [1957] and confirmed by numerous laboratory tests

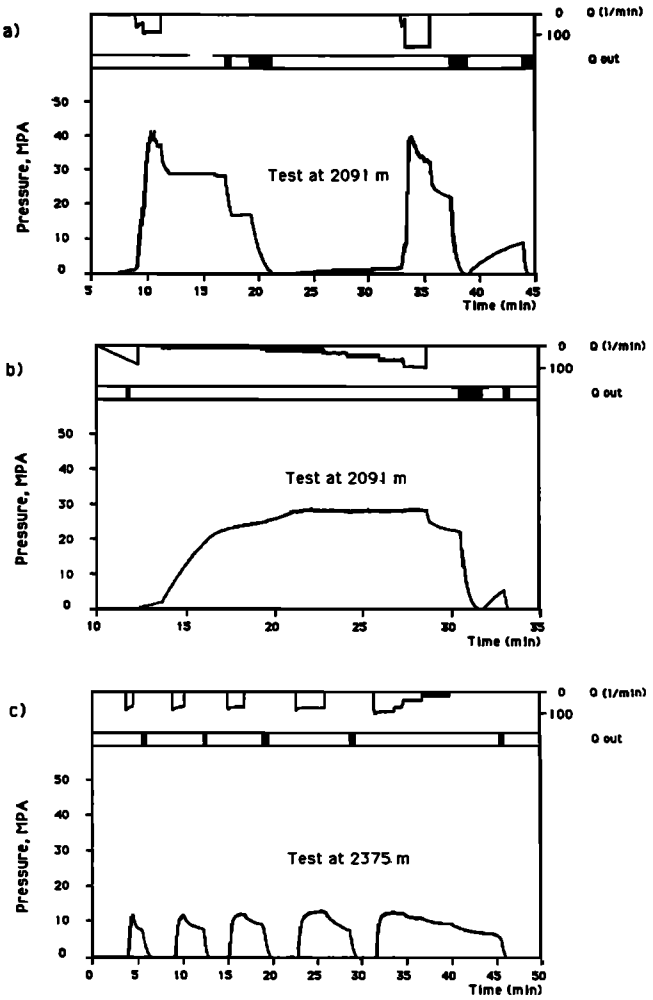

Fig. 4. Pressure and flow data for two hydrofracs in the vicinity of stress anomalously high values of $S_{h\min}$ at about 2100 m. In each figure, the bottom panel shows surface pressure as a function of time, the top panel shows injection rate into the hole and the center panel indicates periods during which flow was allowed to return from the well. Note that the pressure and flow axes are the same in each figure but the time axes are different. (*a*) and (*b*) The last three pressurization cycles from the test at 2091 m and (*c*) the five pressurization cycles for the test at 2375 m.

[e.g., *Haimson and Fairhurst*, 1967, 1970]. Under ideal circumstances excellent correlations between hydrofrac- and strain relief-determined values of $S_{H\max}$ have been obtained (see review of six case histories by *Haimson* [1983]). Nevertheless, even when breakouts and preexisting fractures are absent and best available evidence suggests that one principal stress is parallel to the borehole and the rock surrounding the borehole can be considered both elastic and isotropic, there are still two serious areas of uncertainty in determining $S_{H\max}$ from hydrofrac tests. One involves knowing the appropriate value of tensile strength to use in the hydrofrac breakdown equation [*Bredehoeft et al.*, 1976; *Alexander*, 1983; *Ratigan*, 1983; *Hickman and Zoback*, 1983; *Rummel and Hansen*, 1989]. The other involves the proper manner for incorporating intergranular pore pressure (P_p) on the breakdown, or fracture initiation, pressure (P_b) in low-porosity crystalline rocks [*Rummel et al.*, 1983; *Pine et al.*, 1983; *Schmitt and Zoback*, 1988; *Baumgärtner et al.*, 1990].

These uncertainties are easily seen in the three simple equations that have been used for estimation of $S_{H\max}$ from hydrofrac tests:

$$P_b = 3\ S_{h\min} - S_{H\max} + T - P_p \quad (1)$$

$$P_r = 3\ S_{h\min} - S_{H\max} - P_p \quad (2)$$

$$P_b = 3\ S_{h\min} - S_{H\max} + T \quad (3)$$

Equation (1) is the basic hydrofrac breakdown equation derived from *Haimson and Fairhust* [1967] after *Hubbert and Willis* [1957] for a porous rock in which the fluid pressurizing the borehole does not permeate the formation. As alluded to above, this equation has been used widely and gives excellent results in many cases, although it is often unclear what value for tensile strength should be used in (1). This is because core may not be available for laboratory testing or one is concerned about issues such as scale effects that might make direct application of the laboratory tests questionable [e.g., *Ratigan*, 1983]. Because of these problems, *Bredehoeft et al.* [1976] proposed use of (2) where P_r is the fracture reopening pressure, the pressure at which a hydrofrac opens after it has already been initiated. This method has been widely used and also frequently gives quite reasonable values for the estimated magnitudes of both tensile strength (i.e., $T = P_b - P_r$) and $S_{H\max}$ (see *Bredehoeft et al.* [1976], *Haimson* [1989], *Hickman and Zoback* [1982], *Rummel et al.* [1983], *Tsukahara* [1983], and various papers cited by *Haimson* [1989]).

Hickman and Zoback [1983] discussed methods for determination of accurate values of P_r at length and show that reliable values of P_r can be determined (1) when the fracture reopening pressure is clearly greater than $S_{h\min}$ or (2) during constant injection rate tests, when the volume of fluid in the hydrofrac system has such high "stiffness" that the effect of the volume increase associated with the fracture opening on the pressurization rate is measurable. Unfortunately, these two conditions are not always met. When P_r is less than or approximately equal to $S_{h\min}$, considerable uncertainty can occur in identifying the pressure at which the fracture reopens [see *Hardy and Asgian*, 1989; *Cheung and Haimson*, 1989]. Also, in deep wells such as Cajon Pass, the total volume of fluid in the system is so large that the influence of the hydrofrac opening on the pressurization rate is quite low and P_r can be hard to detect due to the low system stiffness [see *Baumgärtner and Zoback*, 1989].

For these reasons, we decided not to use fracture reopening pressures and (2) for the computation of $S_{H\max}$ in this study. As all of the hydrofracs were performed in crystalline rocks of granodioritic composition, we use an estimate of tensile strength based on the results of laboratory tests and granodiorite core samples and allow considerable variability of the possible value of T. Hydrofrac tests on core sample (D. Schmitt and M. D. Zoback, unpublished data, 1990) indicate an average tensile strength of 11 MPa. We have used $T = 8 \pm 7$ MPa for analysis of these tests to bracket representative and reasonable tensile strengths for this type of rock and to accommodate possible scale effects, recognizing that laboratory measurements on relatively small core samples represent upper bound estimates of tensile strength. While ± 7 MPa causes some degree of uncertainty in the computed values of $S_{H\max}$, this uncertainty is less than 10% of the vertical stress in the lower parts of the hole.

An even more important issue than tensile strength in the accurate computation of $S_{H\max}$ is how to handle intergranular pore pressure, P_p, and whether one should use (1) or (3) in crystalline rock with extremely low porosity. A number of investigators [*Rummel et al.*, 1983; *Pine et al.*, 1983; *Baumgärtner et al.*, 1990] have suggested that in such cases, (3) should be used which neglects intergranular pore pressure on the state of effective stress around the borehole. There is substantial empirical evidence suggesting the validity of (3) in low-porosity crystalline rock. For example, in a number of cases, hydraulic fracturing calculations with (1) in low-porosity crystalline rocks yields computed magnitudes of $S_{H\max}$ that are clearly unreasonable (i.e., $S_{H\max} < S_{h\min}$) whereas when (3) is used not only are the values of $S_{H\max} > S_{h\min}$, but $S_{H\max}$ has values consistent with independent information on the stress state from the style of faulting. This was found to be the case with hydrofrac stress measurements to 2.5 km depth in granitic rocks in Cornwall [*Pine et al.*, 1983] to 3.0 km depth in gneissic rocks in the KTB borehole in southeastern Germany [*Baumgärtner et al.*, 1990] and in many shallow boreholes in crystalline rocks in central Europe [*Rummel et al.*, 1983] and Australia (J. Enever, personal communication, 1989).

To further demonstrate that (3) may be valid for hydraulic fracturing in extremely low-permeability rock, *Schmitt and Zoback* [1989] derived the following two generalized formulas for hydraulic fracture initiation by allowing for the possibility that tensile failure of extremely low-porosity rocks might not be a function of effective stress (the total stress minus the pore pressure):

$$P_b = 3S_{h\min} - S_{H\max} + T - \beta P_p \tag{4}$$

$$P_b = \frac{3S_{h\min} - S_{H\max} + T - \alpha(1-2\nu)/(1-\nu)P_p}{1 + \beta - \alpha(1-2\nu)/(1-\nu)} \tag{5}$$

where α is the Biot coefficient ($\alpha = 1 - K_b/K_m$), K_b is the bulk modulus of the rock aggregate, K_m is the bulk modulus of the mineral grains, ν is Poisson's ratio, and β is defined as a parameter describing the degree to which tensile failure could deviate from a simple effective stress law (i.e., it is assumed that for tensile failure $\sigma_{ij} = S_{ij} - \delta_{ij}\beta P_p$, where δ_{ij} is the Kronecker delta). It is required that $0 < \beta < 1$.

As in the cases of (1)–(3), equation (4) assumes that no fluid penetration from the borehole into the rock occurs prior to fracture initiation, whereas (5) allows for the possibility of fluid permeation into the formation prior to breakdown. When $\beta \sim 1$, as would be expected for porous permeable rocks, (5) is the same as a formula derived by *Haimson and Fairhurst* [1967] to account for fluid permeation effects during hydraulic fracturing. When $\beta \sim 0$, (4) is identical to (3). Values of $\beta \sim 0$ could occur in extremely low-porosity rock due to processes such as dilatancy hardening. It is well known that in triaxial compressive strength tests on saturated crystalline rocks at elevated pore pressure, the influence of pore pressure on strength is negligible at relatively high strain rates because dilatancy prior to failure drops the intergranular pore pressure faster than permeation can restore it [*Brace and Martin*, 1968]. When an extremely low porosity/low-permeability rock fails in tension at a high strain rate (as in a hydrofrac test), dilatancy hardening would also be expected. In fact, *Schmitt and Zoback* [1990] have found evidence of dilatancy hardening in laboratory hydrofrac tests on low porosity crystalline rock. *Morrow and Byerlee* [1988, this issue] point out that because of extensive secondary mineralization, the porosity and permeability of the Cajon Pass core samples are much lower than that of rocks of generally similar composition obtained from the surface. The low permeability of the Cajon Pass samples and the likely sealing of the microcracks adjacent to the borehole by a "mud-cake" argue argue for use of (4). However, even if some fluid penetration did occur prior to breakdown and (5) was more appropriate, $K_b \sim K_m$ and thus $\alpha \sim 0$ in extremely low-porosity crystalline rocks under appreciable confining pressure (such as those hydraulically fractured in the Cajon Pass borehole). Thus it is quite reasonable that both α and β would be close to 0 when a low porosity/low permeability crystalline rock fails in tension in which case both (4) and (5) approach (3).

We find the sum of these arguments and the empirical results of previous investigators compelling and, because we also find that $S_{H\max} < S_{h\min}$ for several of the hydrofracs in the Cajon pass borehole if (1) is used, we follow *Pine et al.* [1983] and *Baumgärtner et al.* [1990] and utilize (3) for computation of $S_{H\max}$, recognizing that this tends to be an upper bound estimate. As discussed by *Vernik and Zoback* [this issue] and shown below, utilization of (3) for the analysis of the hydrofrac data also yields $S_{H\max}$ values closer to those implied by analysis of stress-induced breakouts.

Table 1 and Figure 3 present the data on the magnitude of $S_{H\max}$ determined both by the hydrofrac tests and from the analysis of breakouts of *Vernik and Zoback* [this issue]. While 10 hydrofrac measurements were made in relatively ideal intervals (Table 1), estimates of $S_{H\max}$ are reported for only six depths because in four of the tests equipment problems (or some other factor) complicated the determination of the pressure at which fracture initiation occurred. As noted above, the hydrofrac- and breakout-determined values of $S_{H\max}$ are similar although it is difficult to compare the two sets of values in detail. The two types of data compare quite well between 2000 and 2100 m and the hydrofrac-determined $S_{H\max}$ values at about 2650 m are also comparable to the nearby breakout-determined values. Overall, while the uncertainties for both the hydrofrac- and breakout-determined $S_{H\max}$ values are fairly high, the data indicate that $S_{H\max}$ has a value approximately equal to, to slightly greater than, the vertical stress and increases with depth at a rate similar to that of the vertical stress.

The only value of $S_{H\max}$ that is significantly lower than the vertical stress is at 1277 m in the Arkoma well. This test is somewhat unusual because of an extremely high value of the breakdown pressure. The pressure record for this test [see *Healy and Zoback*, 1988] indicates that the apparent tensile strength for this test is about twice that indicated by the laboratory tests on core samples. If we were to use a higher value of T in the calculations of $S_{H\max}$, its value would be similar in relative magnitude to that indicated by the other shallow measurements in the Arkoma hole (i.e., close to the lithostat).

Stress orientations. As shown in Figure 1, the average direction of the San Andreas fault in the region of Cajon Pass is N60°W. *Shamir and Zoback* [this issue] show that the average direction of maximum horizontal stress determined from the ubiquitous breakouts in the lower half of the DOSECC borehole is N57°E ± 19°. As indicated in Figure 2 and Table 1, the hydrofracs that were detected in the Cajon

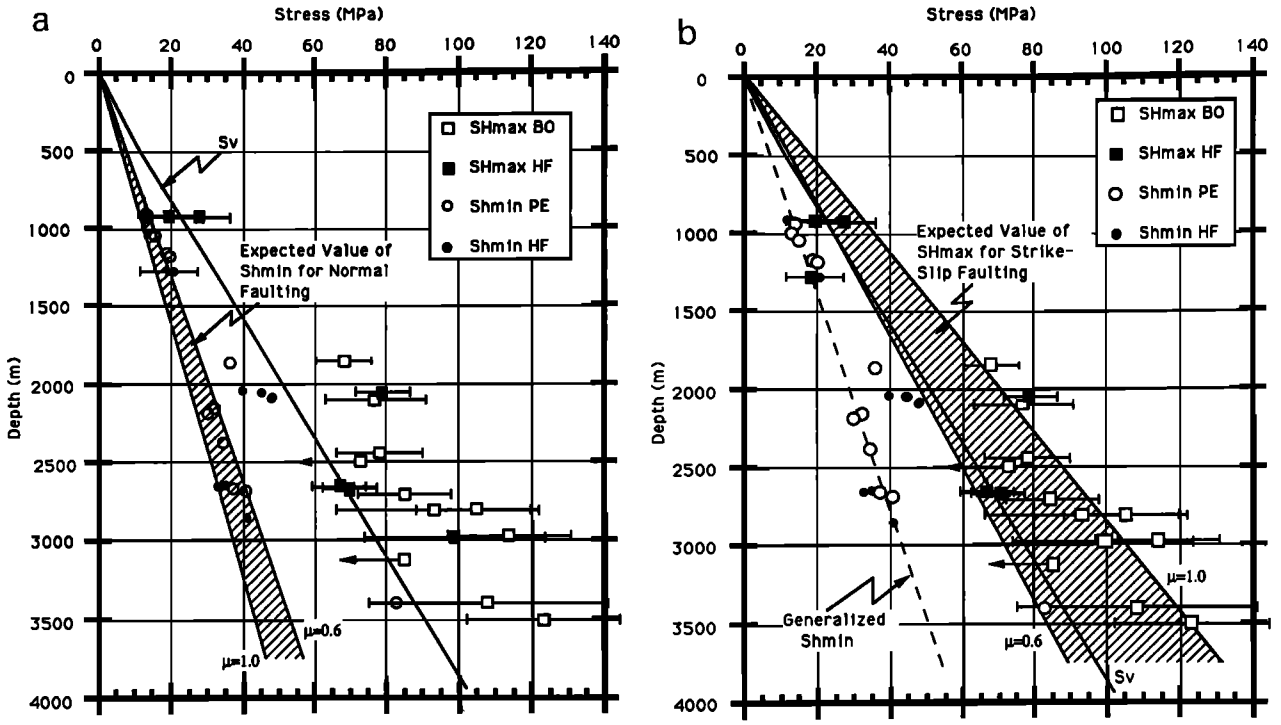

Fig. 5. Data on $S_{h\min}$ and $S_{H\max}$ (same symbols as Figure 3) compared with the theoretical magnitudes predicted using (4) and Byerlee's law (coefficients of friction, m, that range between 0.6 and 1.0) which are indicated by the hachured areas. (*a*) shows the expected value for $S_{h\min}$ for the case of normal faulting ($S_1 = S_v$ and $S_3 = S_{h\min}$). (*b*) shows the expected value for $S_{H\max}$ for the case of strike-slip faulting ($S_1 = S_{H\max}$ and $S_3 = S_{h\min}$) utilizing generalized values for $S_{h\min}$ given by the dashed line in the figure.

Pass borehole are essentially orthogonal to the breakouts in the same or nearby zones. As mentioned above, the excellent correlation of horizontal principal stress orientations inferred from hydraulic fracture orientations and breakout azimuths in numerous case studies led us to rely on breakouts for stress orientation in the Cajon Pass borehole because of the expense and difficulty associated with using impression packers at great depth. While the only comparisons between hydrofrac and breakout orientations that we have in the Cajon Pass well come from a limited range of depths in the hole where the maximum horizontal stress orientation is somewhat anomalous (approximately E-W) with respect to the overall average direction, there is no reason to suspect that the breakouts at other depths are not accurately indicating the directions of horizontal principal stresses.

Discussion

Byerlee's law. As noted in the introduction, nearly all relatively deep in situ stress measurements indicate that stress magnitudes are in general agreement with frictional faulting theory and Byerlee's law. Of comparable depth to the Cajon Pass borehole, the hydrofrac stress measurements of 2.5 km depth in granitic rocks in Cornwall, England indicate a strike-slip faulting stress regime [*Pine et al.*, 1983], those to 3.0 km depth in gneissic rocks in the southeastern Germany [*Baumgärtner et al.*, 1990] indicate a normal/strike-slip faulting stress regime near the bottom of the hole and a similar state of stress exists at ~3.5 km depth in hole EE-2 at Fenton Hill, New Mexico [*Barton et al.*, 1988]. In each case, the measured state of stress is consistent with that informed from earthquake focal plane mechanisms and support the concepts that (1) stress magnitudes in the crust are in equilibrium with the frictional strength of the crust and (2) laboratory-derived coefficients of fraction, μ, in the range of 0.6–1.0 [*Byerlee*, 1978] can be applied to faults in situ. Another way of saying this is that the maximum stress differences in the crust are controlled by the frictional strength of those faults that are most favorably oriented to the principal stress field (i.e., those whose normal is oriented at an angle of $(45° - 0.5 \tan^{-1} \mu)$ to the maximum principal stress [*Jaeger and Cook*, 1971]).

In Figures 5*a* and 5*b* we show that the same thing is generally true for the majority of data collected in the Cajon Pass well. Numerous fault planes cut through the Cajon Pass well at a wide-variety of orientations [*Barton and Zoback*, this issue]. If the ratio of shear to normal stress on favorably oriented fault planes is consistent with predictions based on Mohr-Coulomb theory, it is possible to compare principal stress magnitudes with the following equation from *Jaeger and Cook* [1972] (see also *Zoback and Hickman* [1982], *McGarr et al.* [1982], *Zoback and Healy* [1984], *Stock et al.* [1985], and *Evans and Engelder* [1989]):

$$(S_1 - P_p)/(S_3 - P_p) = [(\mu^2 + 1)^{1/2} + \mu]^2 \qquad (6)$$

Pore fluid pressures in the fractured rock mass drilled at Cajon Pass were found to be very close to hydrostatic [*Coyle and Zoback*, 1988], and we utilize a hydrostatic pore pressure in (6).

For the case of normal faulting, $S_1 = S_v$ and $S_3 = S_{h\min}$. In Figure 5*a* we show the range of expected values of $S_{h\min}$ based on (4) using an estimate of the vertical stress based on

rock densities, coefficients of friction between 0.6 and 1.0 and hydrostatic fluid pressure. With the exceptions of the anomalously high values of $S_{h\min}$ at 2.1 km at 3.5 km noted above, the measured values of $S_{h\min}$ are in agreement with those predicted by (6). In other words, the difference between S_v and $S_{h\min}$ is large enough to make favorably oriented normal faults move. $S_{h\min}$ could have larger values than those predicted by (6) (as is the case with the anomalies at about 2100 m and near the bottom of the hole) because this corresponds to lower shear stress on favorably-oriented fault planes. The values of $S_{h\min}$ cannot be much lower than that predicted by (6) because the shear stress would exceed the frictional strength of favorably-oriented faults. In Figure 5*b*, we show that the same thing is true for the case of strike-slip faulting ($S_1 = S_{H\max}$ and $S_3 = S_{h\min}$) if we utilize a generalized increase of $S_{h\min}$ with depth as shown by the dashed line in the figure. Thus Figure 5 shows that the magnitudes of stresses measured in the Cajon Pass well are in agreement with Mohr-Coulomb theory and Byerlee's law and imply that favorably oriented normal faults and strike-slip faults in the region are expected to be active. In the context of the "strong crust/weak transform" concept for the mechanics of the San Andreas system alluded to above, these data clearly seem to provide evidence for a strong crust adjacent to the San Andreas fault.

The use of hydrostatic fluid pressure in (6) to compute the likelihood of frictional sliding on favorably oriented fault planes is not inconsistent with utilization of zero pore pressure in (3) to relate the pressure of hydraulic fracture initiation to the principal stresses. Utilization of hydrostatic pore pressure in (6) is appropriate because such pressures are consistent with measured values for a ~300-m-long interval of fractured rock at ~2 km in the borehole [*Coyle and Zoback*, 1988]. Thus such pore pressures are presumably acting within potentially active faults and fractures. These same two assumptions, that hydrostatic pore pressure effects frictional failure on preexisting faults but pore pressure does not affect hydraulic fracture initiation, were also made by *Pine et al.* [1983] and *Baumgärtner et al.* [1990], in the two most comparable studies to Cajon Pass conducted to date.

Shear stresses resolved onto the San Andreas fault. In marked contrast to the high shear stresses resolved on favorably oriented faults in the crust penetrated by the Cajon Pass borehole, the abundant data on the orientation of $S_{H\max}$ from the orientations of the well bore breakouts over the entire lower half of the borehole indicates that there is no right-lateral shear stress resolved on planes parallel to the San Andreas fault [see *Shamir and Zoback*, this issue]. Figure 6 combines the data on stress magnitude and orientation in Table 1 and presents computed upper bound values of shear stress parallel to the San Andreas as a function of depth in the well and compares it the expected values of shear stress if Byerlee's law applied to the San Andreas and the normal stress acting on the fault was approximately equal to the vertical stress. As alluded to above, the Cajon Pass site is along a section of the San Andreas which has not had a major earthquake since 1820 and is thus apparently quite "late" in the earthquake cycle. If Byerlee's law applied to the San Andreas, the expected values of right lateral shear would be similar to those in the shaded area. The vertical line at 20 MPa of right-lateral shear indicates the approximate upper bound of average shear stress allowed by

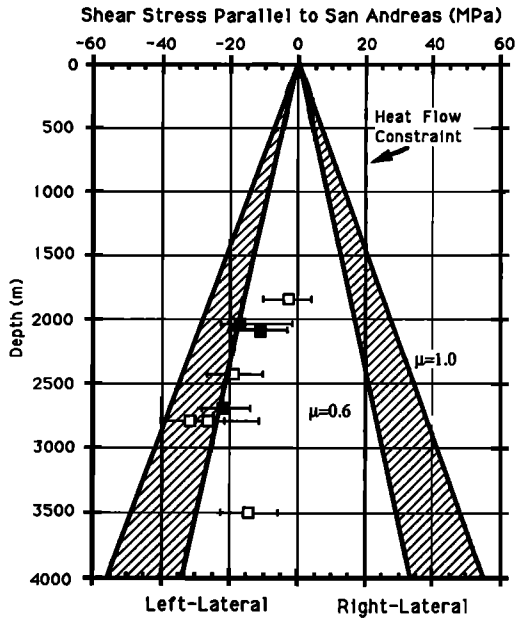

Fig. 6. An upper bound estimate of horizontal shear stresses resolved onto planes parallel to the local strike of the San Andreas fault (right-lateral shear is positive) utilizing the values of $S_{h\min}$ and $S_{H\max}$ and the orientation of principal stresses listed in Table 1. Expected values of right-lateral shear based on Byerlee's law is indicated by the hachured area. The upper limit to average right-lateral shear stresses based on the lack of frictionally-generated heat (~20 MPa [*Lachenbruch and Sass*, 1981]) is also shown. Symbols are the same as in Figures 3 and 5. As the average direction of maximum horizontal compression in the borehole indicates left-lateral shear on planes parallel to the San Andreas, the expected value of shear stress required to cause left-lateral strike-slip movement utilizing Byerlee's law is also shown in the figure.

shallow heat flow data along the San Andreas [*Lachenbruch and Sass*, 1980, 1981].

Figure 7 shows the average orientation of maximum horizontal stress in the Cajon Pass borehole. The shaded range of angles in the figure indicates the ±19° standard deviation of the breakout measurements [*Shamir and Zoback*, this issue]. Thus, within one standard deviation, the stress orientation data indicate fault normal compression to left-lateral shear on planes parallel to the San Andreas, a result inconsistent with the applicability of conventional faulting theory to the San Andreas and its long-term slip history, along both its entire length and at the Cajon Pass site in particular [*Sieh*, 1978; *Weldon*, 1986; *Sieh et al.*, 1989].

Comparison with geology. As pointed out by *Weldon and Springer* [1988], even though the NE-SW orientation of maximum principal stress in the Cajon Pass borehole is inconsistent with right-lateral shear along the San Andreas, it is consistent with the orientation of active strike-slip and normal faults in the immediate vicinity. In this section, we briefly investigate the potential for activity of the secondary faults in the region of the drillsite in the context of the measurements of both stress orientation and magnitude at depth.

The mapping of *Weldon* [1986] and *Matti et al.* [1985] shown in Figure 1*a* illustrates that the Cajon Pass drill site is near the northwestern end of a large region where the style of secondary faulting near the San Andreas is extensional. In the discussion above concerning the consistency of measured stress magnitudes in the borehole with Byerlee's law

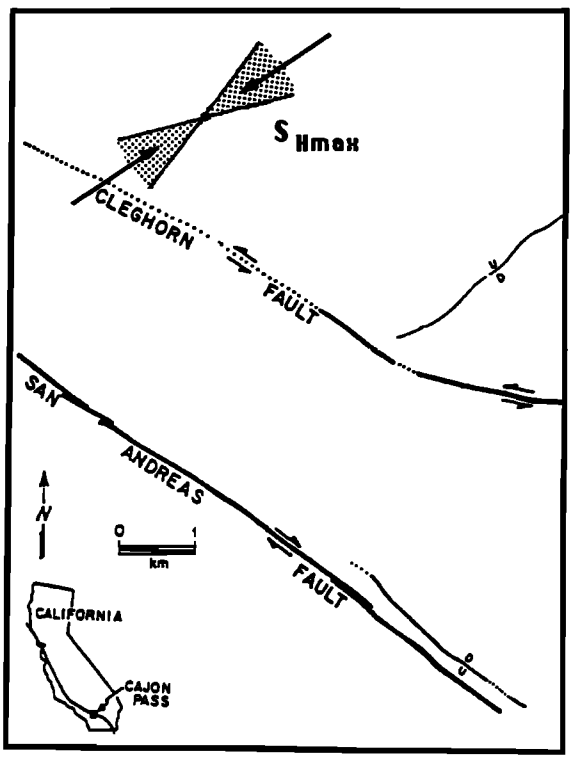

Fig. 7. Active faults in the immediate vicinity of the Cajon pass drill site (modified from *Weldon* [1986] and *Pezard et al.* [1988]) and the average direction (and standard deviation) of maximum horizontal principal stress in the Cajon pass borehole [*Shamir and Zoback*, this issue].

for the crust penetrated by the borehole, we argued that both favorably oriented normal faults and strike-slip faults are potentially active in the vicinity of the Cajon Pass drill site. The likelihood of left-lateral strike-slip faulting on the Cleghorn fault is especially interesting. As mentioned above, it is mapped as a left-lateral strike-slip fault striking subparallel to the San Andreas (Figure 7) near the drill site. We can evaluate the potential for left-lateral slip along the Cleghorn fault by simply considering the amount of left-lateral shear stress resolved onto it. As shown in Figure 6, this is approximately equal to that required to cause left-lateral slip for coefficients of friction of 0.6–1.0 at depths of ~2–3 km. Thus, as implausible as left-lateral slip on the Cleghorn near the San Andreas at Cajon Pass would seem to be, left-lateral slip is consistent with the state of stress measured in the borehole in terms of Byerlee's law. Thus both the stress orientation and stress magnitude data in the Cajon Pass borehole indicate a stress state that is generally consistent with the general style of faulting in the region, especially the left-lateral strike-slip motion on the Cleghorn fault. While no normal faults striking approximately N60°E (as predicted by the borehole measurements) have been mapped in the immediate area of the drillsite, an active, steep, dip-slip fault striking about N60°E was mapped by Meisling and Weldon [1989] only about 3 km east of the drillsite (see Figure 7). Although it is not clear from field relations that this is an active normal fault, it is reasonable to speculate that it is as it is within the extensional domain near the San Andreas mapped by *Weldon* [1986] and *Matti et al.* [1985].

Three hypotheses of the origin of contemporary left-lateral shear and deformation at the Cajon Pass site are offered by *Meisling and Weldon* [1989], *Saucier et al.* [this issue] and *Shamir* [1990]. Meisling and Weldon suggest that the style of geologic deformation is largely the result of the complexities in the three-dimensional shape of the San Andreas. They argue that in addition to variations in strike observable in Figure 1*a* and 7, the San Andreas dips to the northeast in the Cajon Pass region and that the subsurface trace of the fault may be offset to the northeast by several kilometers [see *Meisling and Weldon*, 1989, Figure 15]. To explain patterns of geologic deformation observed at the surface in the western San Bernadino mountains and the Cajon Pass area, they argue that the movement of mass around this "bulge" at depth results in the uplift and extension. Saucier et al. suggest that right-lateral slip associated with bends in an essentially vertical San Andreas fault plane introduce areas of concentrated left-lateral shear and extension in the Cajon Pass area that are generally consistent with the region in which such deformation is mapped. For the case when the right-lateral slip relieves all of the right-lateral shear (i.e., a weak fault) left-lateral shear stresses can accumulate over several earthquakes until they can eventually cause secondary crustal deformation. *Shamir* [1990] suggested that the left lateral shear might be the result of dynamic stress redistributions in the 1812 earthquake which are somewhat intensified by geometric effects like those studied by Saucier et al. He pointed to examples of left-lateral strike-slip aftershocks on planes parallel to the San Andreas that occurred after the 1966 Parkfield earthquake as a possible analog to what might be the cause of what is observed at Cajon Pass today.

The consistency between the normal/strike-slip fault in stress regime indicated by geologic deformation in the region of the drill site and the stress magnitude measurements in the Cajon Pass borehole seem to add appreciably to the arguments based on the orientation of the in situ stress field and strikes of secondary faults made by *Weldon and Springer* [1988]. There is indeed an excellent correlation between the state of stress and style of geologic deformation in the region in the immediate vicinity of the drill hole. Nevertheless, the map of active faults in the Cajon Pass region clearly shows that one would expect that the direction of maximum horizontal compression and relative magnitudes of principal stresses would change spatially. To a degree this is also reflected in earthquake focal plane mechanisms along the San Andreas [*Jones*, 1988]. To the northwest of Cajon Pass there is a region where the state of stress is compressional (see for example the active thrust fault that is mapped near the San Andreas close to Pallett Creek in Figure 1*a*). Stress measurements made at a site called Crystallaire (4 km northeast of the San Andreas near Pallett Creek) to almost 1 km depth found a reverse faulting stress state in the upper ~300 m and a strike-slip faulting stress regime at greater depth with a direction of maximum horizontal compression ~N20°W [*Zoback et al.*, 1980]. To the southeast of the drill site along the San Andreas, earthquake focal plane mechanisms define the extensional stress state near the San Andreas defined by the mapping of *Weldon* [1986] and *Matti et al.* [1985]. Thus both earthquake focal plane mechanisms [*Jones*, 1988] and the style of secondary crustal deformation imply that the state of stress changes markedly along the strike of the San Andreas system in southern California. There remains a discrepancy between the stress orientation

at Cajon Pass and that in the adjacent regions as indicated by earthquake focal plane mechanisms near the San Andreas. The strike-slip/reverse faulting earthquakes to the northwest in the Pallett Creek/Crystallaire area and the strike-slip/normal faulting earthquakes to the southeast both have NNW trending P axes [*Jones*, 1988]. This discrepancy may simply be the result of sampling a nonuniform stress field along the fault (see also the discussion by *Shamir and Zoback* [this issue]). As shown by *Jones* [1988, Figure 13], there are no well-constrained earthquake focal plane mechanisms that are within ±10 km of the San Andreas directly within the domain defined by the Cleghorn fault and drill site (the area to adjacent to the northwest side of the San Andreas in the westernmost San Bernadino mountains).

One could argue that the stress orientation observed in the Cajon Pass borehole and the changes in deformational style along the strike of the San Andreas indicated by active secondary faults shown in Figure 1*a* simply reflect superficial features that are perhaps related to a weak San Andreas at shallow depth but are not really indicative of the level of shear stress on the fault at seismogenic depth. An obvious problem with such arguments is that they clearly violate constraints on frictional stress imposed by heat flow measurements along the length of San Andreas (and in the Cajon Pass borehole in particular [*Lachenbruch and Sass*, this issue]). The lack of frictionally generated heat along the San Andreas argues that the fault must be weak, especially below 5 km. If the frictional strength of the San Andreas was zero from the surface to a depth of about 5 km but consistent with Byerlee's law from 5 to 15 km, it would only diminish the average frictional resistance on the fault by about 10% (for an average increase of frictional resistance of about 10 MPa/km), not the decrease of frictional resistance of a factor of 3–5 was required by the heat flow data. Moreover, the state of stress and style of secondary deformation observed throughout the Coast Ranges in central California appear to change neither with depth nor distance from the fault (compare the breakout and focal plane mechanism data in Figure 1 of *Zoback et al.* [1987]).

The state of stress throughout southern California is clearly more complex than that in central California. Nevertheless, the angles between the local strike of San Andreas and the $S_{H\max}$ directions inferred from the focal plane mechanism inversions near it do indicate that the frictional strength of the fault is low [*Jones*, 1988] from Fort Tejon to Indio. Moreover, while earthquake focal plane mechanisms near the San Andreas and in the Los Angeles basin show ~N-S compression [*Hauksson*, 1990], compression nearly perpendicular to the San Andreas is observed at distances more than 10 km away from the fault is indicated by a number of focal plane mechanisms in the eastern Transverse Ranges [*Webb and Kanamori*, 1985] and by well bore breakout data and earthquake focal plane mechanisms along the coast [*Zoback et al.*, 1987; *Hauksson*, 1990].

Finally, we should address the possibility that the overall state of stress in the upper 3.5 km at the Cajon Pass site might be affected by some large-scale perturbations of the regional stress field. Two such perturbations of the stress field are those associated with topography and the great 1857 Fort Tejon earthquake, which broke to within about 20 km of Cajon Pass to the northwest. Three other papers in this issue deal with these questions in some detail. Both *Saucier et al.* [this issue] and *Shamir and Zoback* [this issue] model stress changes associated with the 1857 earthquake. For smoothly decaying slip at the southern end of the rupture, both studies showed that the 1857 rupture had negligible effect on the current state of stress at Cajon Pass. Shamir and Zoback also showed that no marked changes of stress magnitude would occur in the upper 7–8 km at the Cajon Pass site as a result of the long-term cycle of stress accumulation and release along the San Andreas and San Jacinto faults. *Liu and Zoback* [this issue] describe a new method for modelling three-dimensional topography and apply it to computing effects of topography in the San Gabriel and San Bernadino mountains on state of stress at depth in the Cajon Pass area. They show that topographic effects also have a negligible effect on the measures stress magnitudes and orientations in the borehole at depths greater than 1–2 km.

Another type of stress perturbation that could affect the stress measurements are the stress drops associated with slip on the numerous minor faults in the area and especially those that cut directly through the well. *Shamir and Zoback* [this issue] point out evidence in the borehole for perturbations of the stress field associated with slip on such faults at a variety of scales. It is unlikely, however, that this phenomena could effect the overall state of stress measured in the borehole. As shown in Figure 7 and discussed above, the state of stress measured in the Cajon Pass borehole is consistent with the style of faulting in the region, and it is clear that the borehole is sampling a "stress domain" characteristic of a fairly large area adjacent to the San Andreas. Even at the relatively modest depth of 3.5 km reached, right-lateral shear stresses should be about 30–50 MPa if Byerlee's law and hydrostatic pore pressures were relevant to the San Andreas (e.g., Figure 6). As such shear stresses are much larger than the ~1–10 MPa average stress drops of large earthquakes, and it would take an extremely large stress drop over an extremely large fault area to affect the overall state of stress in the entire region in which the borehole is located.

Overall, the excellent correlation between the style of local faulting and the stress measurements made in the borehole indicates that the remarkable thing about the stress measurements in the Cajon pass borehole is that there are no surprises if we forget about the San Andreas fault. *Lachenbruch and Sass* [this issue] reached the same conclusions based on their thermal studies to 3.5 km depth as did *Healy and Zoback* [1988] after stress measurements were made to 2.1 km. In the introduction we referred to the two hypotheses Healy and Zoback proposed to explain the state of stress and style of geologic deformation around the well site: either the crust in the region of the borehole was decoupled from the San Andreas or the San Andreas is quite weak. The fact that a complete absence of right-lateral shear on planes parallel to the San Andreas is observed to 3.5 km suggests that both of these hypotheses may be correct.

Stress perturbations. It is interesting to briefly speculate about possible causes of the two localized zones where the last principal stress markedly deviates from the magnitudes consistent with Byerlee's law and increases in the Cajon Pass well to values close to that of the overburden stress (Figure 5*a*). Two other wells drilled in areas of active normal faulting in situ stress measurements are known to show similar phenomena. In four wells on the Nevada Test Site near Yucca mountain, *Stock and Healy* [1988] show that nearly all the last principal stress values are consistent with predicted values based on Byerlee's law for an area of active

normal faulting (and are thus considerably less than the vertical stress). However, in two of the wells, USW G-2 and Ue25P1, localized increases of $S_{h\min}$ are observed where the values deviate from Byerlee's law and reach values close to the vertical stress. The same thing was observed with stress measurements made in borehole SST-701 drilled in 6th Water canyon, Utah (U.S. Bureau of Reclamation, unpublished memorandum, 1990). In fact, the similarities of the state of stress, magnitude of stress perturbations and style of local faulting among these two cases and the Cajon Pass data are striking.

Shamir and Zoback [this issue] discuss variations of stress orientation with depth in the Cajon Pass borehole that occur at a variety of scales and wavelengths. The best explanation of these variations of stress orientation seems to be that they result from slip (of varying scale) on faults that pass through and near the hole. They argue that the highly faulted nature of the shallow crust in the western Mojave desert seems also to be the most likely explanation for the unusually large degree of variability of stress managements in that region (see also *Hickman* [1991]). We therefore hypothesize that the perturbations in the magnitude of least principal stress with depth may also be the result of slip on active faults that cut through the hole (i.e., we are sampling the perturbations of the stress field associated with past earthquakes). Because $S_1 = S_v$ and $S_3 = S_{h\min}$ in a normal faulting environment, the drop in shear stress in an earthquake must be accompanied by an increase in $S_{h\min}$ because the magnitude of the overburden stress is fixed by the weight of the rock. This is schematically shown in Figures 8*a* and 8*b*. In the vicinity of the stress anomaly at about 2100 m, analysis of borehole televiewer data revealed a fault at a depth of 2038 m. While many faults and fractures cut through the hole in this general depth range, this particular fault appears to be normal fault that is favorably-oriented to the stress field (i.e., it strikes ~E-W, essentially parallel to the direction of maximum principal stress at that depth and dips 60° to the north). To test the plausibility of the hypothesis that slip on such a fault may have caused the stress anomaly observed at about 2100 m in the Cajon Pass borehole, we have modelled the change in the magnitude of least principal stress associated with slip on this fault. To compute the stress changes, we used the program DIS3D [*Erickson*, 1987], which models the stress and displacements associated with dislocations in an elastic half-space.

We show in Figure 8*c* the results of two of the models, 15 cm of offset on a 200 by 200 m fault patch cutting through the well and 30 cm of offset on a 400 by 400 m patch. While such modelling is inherently nonunique, in the context of the model the stress magnitude data do constrain some general characteristics of the slip on the fault hypothesized to have caused the anomaly. Less slip would have produced less of an increase of the magnitude of the least principal stress and slip over a broader area would have produced an anomaly detected over a greater range of depths. The decreases of the magnitude of least principal stress below the values predicted by Byerlee's law (the negative lobes on the stress pertubations) would not be expected to occur in nature as it would result in too much shear stress on favorably oriented normal faults.

Despite the good fit between the models shown in Figure 8*c*, our goal in presenting the modeling is only to argue conceptually that stress anomalies in normal faulting environments such as those encountered in the Cajon Pass borehole (and the other cases described above), may simply be the result of sampling the perturbations of the stress field associated with past earthquakes. If this hypothesis is correct, the stress drop on earthquakes was nearly complete as the least principal stress has a magnitude almost equal to the vertical stress. On the basis of analysis of strong motion seismograms *McGarr* [1981, 1984] has argued that large, near-complete stress drops might occur in the hypocentral zones of earthquakes.

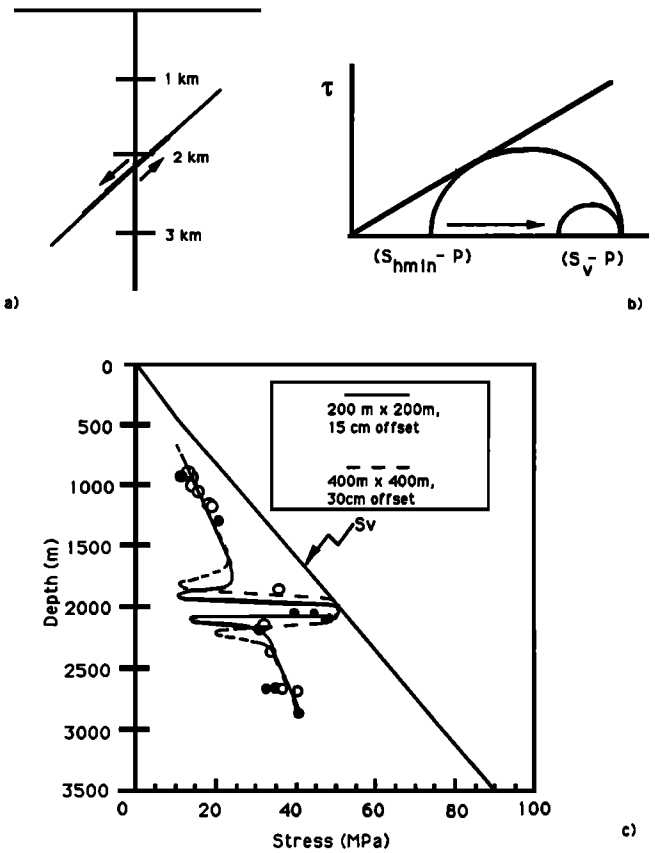

Fig. 8. (*a*) Schematic of normal fault cutting through the borehole at 2038 m which may be related to the increase of least principal stress measured at about that depth. The fault strikes E-W, parallel to the direction of maximum horizontal compression at that depth and dips 60° to the north. (*b*) Mohr diagram illustrating that the drop in shear stress associated with a normal faulting earthquake would require an increase in the magnitude of least effective principal stress. (*c*) Results of dislocation modelling of the stress perturbation associated with normal slip on the fault at 2038 m (see text).

CONCLUSIONS

Measurements of in situ stress orientation and magnitude in the two boreholes drilled at Cajon Pass indicate ratios of shear to normal stress on favorably oriented fault planes consistent with Byerlee's law, i.e., predictions of stress magnitudes based on Mohr-Coulomb theory utilizing laboratory-determined coefficients of friction in the range 0.6–1.0. Twenty-three hydraulic fracturing tests yielded data on the magnitude of the least horizontal principal stress, $S_{h\min}$, from 0.8 to 3.5 km depth. Six estimates of the magnitude of the maximum horizontal principal stress, $S_{H\max}$, were also determined from the hydrofracs, and an additional 12 esti-

mates of $S_{H\max}$ were obtained from analysis of stress-induced well bore breakouts utilizing knowledge of rock strength and the hydrofrac-determined values of least principal stress [*Vernik and Zoback*, this issue]. The consistency of stress magnitudes in the Cajon Pass boreholes with Byerlee's law is similar to results of stress measurements at a number of sites around the world [e.g., *McGarr and Gay*, 1978; *Brace and Kohlstedt*, 1980; *Pine et al.*. 1983; *Zoback and Healy*, 1984; *Stock et al.*, 1985; *Zoback et al.* 1988*a*; *Baumgärtner et al.*, 1990]. As the validity of Byerlee's law is demonstrated for the case of normal faulting by the differences between the vertical stress and nearly all of the least principal stress values, this conclusion is independent of the relatively large uncertainties associated with the $S_{H\max}$ values.

In two places in the borehole, the magnitude of the least principal stress deviates from the values predicted by Byerlee's law for active normal faulting and increases to values approximately equal to the overburden stress. These localized stress perturbations can be modelled as near-complete stress drop associated with slip in past earthquakes with scale dimensions of a few hundred meters that occurred on normal faults that cut through the well.

In marked contradiction to the applicability of Byerlee's law for the crust penetrated by the borehole, abundant data on the orientation of $S_{H\max}$ to 3.5 km depth [*Shamir and Zoback*, this issue] indicate that there is left-lateral and not right-lateral shear stress resolved onto the San Andreas fault in this area. The lack of right-lateral shear stress on the San Andreas is extremely surprising at a site that is presumably quite "late" in the earthquake cycle [*Weldon*, 1986; *Sieh et al.*, 1989]. As surprising as this result is, the low least principal stress and tendency for normal faulting measured in the borehole is consistent with the overall style of active secondary faulting in the region encompassing Cajon Pass and that extending to the southeast [*Weldon*, 1986]. Perhaps more importantly, the state of stress measured in the borehole is consistent with the left-lateral strike slip observed on the Cleghorn fault [*Weldon*, 1986; *Weldon and Springer*, 1988] that is located approximately half way between the drill site and the San Andreas. Even at the relatively modest depth of 3.5 km reached in the Cajon Pass borehole, right-lateral shear stresses should be about 3–50 MPa if Byerlee's law was relevant to the San Andreas [e.g., *Sibson*, 1974]. As such shear stresses are much larger than the ~1–10 MPa average stress drops of large earthquakes, and it would take an extremely large stress drop over an extremely large fault area to negate 30–50 MPa of expected right-lateral shear and affect the overall state of stress in the entire region in which the borehole is located.

It is clear in Figure 1*a* that the style of secondary faulting is quite variable along the San Andreas in southern California. We argue that the only way that such variations of deformational style can exist (especially that left-lateral shear that occurs essentially adjacent to the San Andreas in the Cajon Pass region) is that motion on the San Andreas does not require large magnitude right-lateral shear stresses. It is not possible to say to what depth the observed left-lateral shear in the borehole (and corresponding left-lateral slip on the Cleghorn) might persist. But the consistency between the state of stress measured in the Cajon Pass borehole and the active faulting in the region demonstrates that we are sampling a "stress domain" characteristic of a fairly large area adjacent to the San Andreas (Figure 1*a*). Even at a relatively modest depth of 3.5 km (earthquake focal depths in the region extend from 3.6 to 11.3 km [*Jones*, 1988]), measured right-lateral shear stresses are ~30–50 MPa less than that predicted by conventional faulting theory and Byerlee's law. As this amount is much larger than the ~1–10 MPa average stress drops by large earthquakes, we believe that the style of deformation and the state of stress currently measured in the Cajon Pass/Cleghorn fault region is a persistent feature, relatively unaffected by the stress drops associated with individual earthquakes on the San Andreas or other faults in the region (see also *Saucier et al.* [this issue] and *Shamir and Zoback* [this issue]).

Overall, the in situ stress measurements in the Cajon Pass borehole support the "strong curst/weak transform" conceptual model for faulting along the San Andreas system referred to above that was originally proposed for central California. Heat flow measurements in the Cajon Pass borehole [*Lachenbruch and Sass*, this issue] indicate no evidence of frictionally generated hear from the San Andreas and thus support inferences about the low frictional strength of the fault based on the heat flow measurements in shallow boreholes. Thus both the stress and heat flow measurements to 3.5 km depth in the Cajon Pass borehole support the hypothesis that slip along the San Andreas fault occurs at shear stresses markedly lower than that predicted by conventional faulting theory and laboratory coefficients of friction in the range of 0.6–1.0.

Acknowledgments. Many people deserve thanks for their help with this study. Tom Moses, Jörg Baumgärtner, Joe Svitek, and Brennan O'Neil all provided invaluable help with making the hydrofrac measurements. Jörg is also thanked for performing the interactive analysis of the hydraulic fracturing pressure data. Many of our colleagues at Stanford and the USGS provided further assistance in a variety of ways. We thank Mark Ader and Dennis Styles of the USGS and Colleen Barton, David Castillo, Dan Moos, Doug Schmitt, Gadi Shamir, and Lev Vernik of Stanford for their efforts as well as Robert Johnson of DOSECC for this technical help and advice. We also thank Karl Fuchs, Bezalel Haimson, Art Lachenbruch, Art McGarr, Richard Plumb, and Mary Lou Zoback for their suggestions that improved this manuscript. Funding for this study came from the National Science Foundation Continental Dynamics Program through DOSECC, Inc. and grant NSF-EAR-8916280 and from the USGS Deep Continental Studies Program. This manuscript was written while one of the authors (M.D.Z.) was on sabbatical leave at the University of Karlsruhe, Germany. The financial support of the Alexander von Humboldt Stiftung is gratefully acknowledged.

REFERENCES

Alexander, L., Note on effects of infiltration on the criterion for breakdown in hydraulic fracturing stress measurements, in *Hydraulic Fracturing Stress Measurements*, edited by M. D. Zoback and B. C. Haimson, pp. 143–148, National Academy Press, Washington, D. C., 1983.

Anderson, T. O., and E. J. Stahl, A study of induced fracturing using an instrumental approach, *Soc. Pet. Eng. J.*, *7*, 261–267, 1967.

Barton, C. A., In-situ stress measurement techniques for deep drillholes, Ph.D. thesis, Stanford Univ., Stanford, Calif., 1988.

Barton, C. A., and D. Moos, Natural fractures in the Cajon Pass scientific drillhole and their effect on rock properties, *Geophys. Res. Lett.*, *15*, 1013–1016, 1988.

Barton, C. A., and M. D. Zoback, Self-similar distribution and properties of macroscopic fractures at depth in crystalline rock in the Cajon Pass scientific drill hole, *J. Geophys. Res.*, this issue.

Barton, C. A., M. D. Zoback, and K. T. Burns, In-situ stress orientation and magnitude at the Fenton Hill geothermal site,

New Mexico, determined from well bore breakouts, *Geophys. Res. Lett.*, *15*, 467–470, 1988.

Barton, C. A., L. Tessler, and M. D. Zoback, Interactive analysis of borehole televiewer data, in *Automated Pattern Analysis in Petroleum Exploration*, edited by I. Palaz and S. Sengupta, pp. 217–242, Springer-Verlag, New York, 1991.

Baumgärtner, J., and M. D. Zoback, Interpretation of hydraulic fracturing pressure-time records using interactive analysis methods, *Int. J. Rock Mech. Min. Sci.*, *26*, 461–470, 1989.

Baumgärtner, J., F. Rummel, and M. D. Zoback, Hydraulic fracturing in situ stress measurements to 3 km depth in the KTB pilot hole VB: A summary of a preliminary data evaluation, *KTB Rep. 90-6a*, pp. 353–400, NLfB, Hannover, Germany, 1990.

Bell, J. S., and D. I. Gough, Northeast-southwest compressive stress in Alberta: Evidence from oil wells, *Earth Planet. Sci. Lett.*, *45*, 475–482, 1979.

Bell, J. S., and D. I. Gough, The use of borehole breakouts in the study of crustal stress, in *Hydraulic Fracturing Stress Measurements*, edited by M. D. Zoback and B. C. Haimson, pp. 201–209, National Academy Press, Washington, D. C., 1983.

Bilham, R., and G. King, The morphology of strike-slip faults: Examples from the San Andreas fault, California, *J. Geophys. Res.*, *94*, 10,204–10,216, 1989.

Blümling, P., K. Fuchs, and T. Schneider, Orientation of the stress field from breakouts in a crystalline well in a seismic active area, *Phys. Earth Planet. Sci. Lett.*, *33*, 250–254, 1983.

Brace, W. F., and J. D. Byerlee, Stick-slip as a mechanism for earthquakes, *Science*, *153*, 990–992, 1966.

Brace, W. F., and D. L. Kohlstedt, Limits on lithospheric stress imposed by laboratory experiments, *J. Geophys. Res.*, *85*, 6248–6252, 1980.

Brace, W. F., and R. J. Martin III, A test of the law of effective stress for crystalline rocks of low porosity. *Int. J. Rock Mech. Min. Sci.*, *5*, 415–426, 1968.

Bredehoeft, J. D., R. G. Wolff, W. S. Keys, and E. Shuter, Hydraulic fracturing to determine the regional in situ stress field, Piceance Basin, Colorado, *Geol. Soc. Am. Bull.*, *87*, 250–258, 1976.

Brune, J. N., T. L. Henyey, and R. F. Roy, Heat flow, stress, and rate of slip along the San Andreas fault, California, *J. Geophys. Res.*, *74*, 3821–3827, 1969.

Byerlee, J. D., The mechanics of stick-slip, *Tectonophysics*, *9*, 475–486, 1970.

Byerlee, J. D., Friction of rocks, *Pure Appl. Geophys.*, *116*, 615–629, 1978.

Chen, W. P., and P. Molnar, Focal depths of intracontinental and intraplate earthquakes and their implications for the thermal and mechanical properties of the lithosphere, *J. Geophys. Res.*, *88*, 4183–4214, 1983.

Cheung, L. S., and B. C. Haimson, Laboratory study of hydraulic fracturing pressure data—how valid is their conventional interpretation?, *Int. J. Rock Mech. Min. Sci. Geomech. Abstr.*, *26*, 595–604, 1989.

Cox, J., Long-axis orientation in elongated boreholes and its correlation with rock stress data, *Trans. SPWLA Annu. Logging Symp.*, *24th*, 1983.

Coyle, B. J., and M. D. Zoback, In situ permeability and fluid pressure measurements at ~2 km depth in the Cajon Pass research well, *Geophys. Res. Lett.*, *15*, 1029–1032, 1988.

Dieterich, J., Modeling of rock friction, 1, Experimental results and constitutive equations, *J. Geophys. Res.*, *84*, 2161–2168, 1979.

Ehlig, P. L., Geologic structure in the vicinity of the Cajon Pass scientific drill hole, *Geophys. Res. Lett.*, *15*, 953–956, 1988*a*.

Ehlig, P. L., Characteristics of basement terrane exposed north of the San Andreas fault near the Cajon pass scientific research well, *Geophys. Res. Lett.*, *15*, 949–952, 1988*b*.

Erickson, L., User's manual for DIS3D: A three-dimensional dislocation program with applications to faulting in the Earth, 167 pp., Stanford Univ., Stanford, Calif., 1987.

Evans, K., and T. Engelder, Some problems in estimating horizontal stress magnitudes in "thrust" regimes, *Int. J. Rock Mech. Min. Sci Geomech. Abstr.*, *26*, 647–660, 1989.

Gough, D. I., and J. S. Bell, Stress orientations from oil well fractures in Alberta and Texas, *Can. J. Earth Sci.*, *19*, 1358–1370, 1981.

Gough, D. I., and J. S. Bell, Stress orientations from borehole wall fractures with examples from Colorado, east Texas, and northern Canada, *Can. J. Earth Sci.*, *19*, 1358–1370, 1982.

Haimson, B. C., The hydrofracturing stress measurement technique—Method and recent field results in the US, in *Proceedings of International Society of Rock Mechanics Symposium*, pp. 23–30, Sydney, Australia, 1976.

Haimson, B. C., Crustal stress in the continental United States as derived from hydrofracturing tests, in *The Earths Crust, Geophys. Monogr. Ser.*, vol. 20, edited by J. C. Heacock, pp. 575–592, AGU, Washington, D. C., 1977.

Haimson, B. C., A comparative study of deep hydrofracturing and overcoring stress measurements at six locations with particular interest to the Nevada Test Site, in *Hydraulic Fracturing Stress Measurements*, pp. 107–118, National Academy Press, Washington, D. C., 1983.

Haimson, B. C. (Ed.), Hydraulic fracturing stress measurements, special issue, *Int. J. Rock Mech. Min. Sci. Geomech. Abstr.*, *26*, 1989.

Haimson, B. C., and C. Fairhurst, Initial and extension of hydraulic fractures in rocks, *Soc. Pet. Eng. J.*, *7*, 310–318, 1967.

Haimson, B. C., and C. Fairhurst, In-situ stress determination at great depth by means of hydraulic fracturing, in *11th Symposium on Rock Mechanics*, edited by W. Somerton, pp. 559–584, Society of Mining Engineers of AIME, New York, 1970.

Hanks, T. C., Earthquake stress drops, ambient tectonic stresses and stresses that drive plate motions, *Pure Appl. Geophys.*, *115*, 441–458, 1977.

Hardy, M., and V. Asgian, Fracture reopening during hydraulic fracturing stress determinations, *Int. J. Rock. Mech. Min. Sci. Geomech. Abstr.*, *26*, 489–498, 1989.

Hauksson, E., Earthquakes, faulting and stress in the Los Angeles Basin, *J. Geophys. Res.*, *95*, 15,365–15,394, 1990.

Healy, J., and M. D. Zoback, Hydraulic fracturing stress measurements in the Cajon Pass research well to 2 km depth, *Geophys. Res. Lett.*, *15*, 1005–1008, 1988.

Henyey, T. L., and G. J. Wasserburg, Heat flow near major strike-slip faults in California, *J. Geophys. Res.*, *76*, 7924–7946, 1971.

Herrick, C. G., and B. C. Haimson, Boreholes drilled in rock subjected to far-field stresses: Is there a breakout size-stress relationship?, *Eos Trans. AGU*, *71*, 1621, 1990.

Hickman, S., Stress in the lithosphere and the strength of active faults, U.S. National Report to IUGG 1987–1990, Part 2, *Rev. Geophys.*, *29*, suppl., 759–775, 1991.

Hickman, S. H., and M. D. Zoback, The interpretation of hydraulic fracturing pressure-time data for in-situ stress determination, in *Hydraulic Fracturing Stress Measurements*, pp. 44–54, National Academy Press, Wash., D. C., 1982.

Hickman, S. H., J. H. Healy, and M. D. Zoback, In situ stress, natural fracture distribution, and borehole elongation in the Auburn geothermal well, Auburn, New York, *J. Geophys. Res.*, *90*, 5497–5512, 1985.

Hubbert, M. K., and D. G. Willis, Mechanics of hydraulic fracturing, *J. Pet. Technol.*, *9*, 153–168, 1957.

Jacoby, G. C., P. R. Shepard, and K. E. Sieh, Irregular recurrence of large earthquakes along the San Andreas fault: Evidence from trees, *Science*, *241*, 196–199, 1988.

Jaeger, J. C., and N. G. W. Cook, *Fundamentals of Rock Mechanics*, 3rd ed., 593 pp., Chapman and Hall, New York, 1971.

Jones, L., Focal mechanisms and the state of stress on the San Andreas fault in southern California, *J. Geophys. Res.*, *93*, 8869–8891, 1988.

Kanamori, H., State of stress in the Earth's lithosphere, in *Physics of the Earth's Interior*, pp. 531–554, Societé Italiana di Fisica, Bologna, Italy, 1980.

Kanamori, H., and D. L. Anderson, Theoretical basis of some empirical relations in seimology, *Bull. Seismol. Soc. Am.*, *65*, 1073–1095, 1975.

Kirby, S., Tectonic stresses in the lithosphere: Constraints provided by the experimental deformation of rocks. *J. Geophys. Res.*, *85*, 6353–6363, 1980.

Kirsch, G., Die Theorie der Elastizitat und die Bedurfnisse der Festigkeitslehre, *VDI Z*, *42*, 707, 1898.

Lachenbruch, A. H., and J. H. Sass, Thermo-mechanical aspects of the San Andreas fault system, in *Proceedings of the Conference on Tectonic Problems of the San Andreas Fault System*, edited by

R. L. Kovach and A. Nur, 192–205, Stanford University Press, Palo Alto, Calif., 1973.

Lachenbruch, A. H., and J. H. Sass, Heat flow and energetics of the San Andreas fault zone, *J. Geophys. Res.*, *85*, 6185–6223, 1980.

Lachenbruch, A. H., and J. H. Sass, Corrections to "Heat flow and energetics of the San Andreas fault zone" and some additional comments on the relation between fault friction and observed heat flow, *J. Geophys. Res.*, *86*, 7171–7172, 1981.

Lachenbruch, A. H., and J. H. Sass, The stress heat-flow paradox and preliminary thermal results from Cajon Pass, *Geophys. Res. Lett.*, *15*, 981–984, 1988.

Lachenbruch, A. H., and J. H. Sass, Heat flow from Cajon Pass: Fault strength and tectonic implications, *J. Geophys. Res.*, this issue.

Lachenbruch, A. H., and G. A. Thompson, Oceanic ridges and transform faults: Their intersection angles and resistance to place motion, *Earth Planet. Sci. Lett.*, *15*, 116–122, 1972.

Liu, L., and M. D. Zoback, The effect of topography on the state of stress in the crust: Application to the site of the Cajon Pass scientific drilling project. *J. Geophys. Res.*, this issue.

MacKenzie, D. P., The relationship between fault plane solutions for earthquakes and the directions of the principal stresses, *Bull. Seismol. Soc. Am.*, *59*, 591–601, 1969.

Maloney, S., and P. K. Kaiser, Results of borehole breakout simulation tests, in *Rock at Great Depth*, edited by V. Maury and D. Fourmaintraux, pp. 745–752, A. A. Balkema, Rotterdam, Netherlands, 1989.

Matti, J. C., D. M. Morton, and B. F. Cox, Distribution and geologic relations of fault systems in the vicinity of the central Transverse Ranges, southern California, *U. S. Geol. Surv. Open File Rep.*, *85-365*, 1985.

McGarr, A., Some constraints on levels of shear stress in the crust from observations and theory, *J. Geophys. Res.*, *84*, 6231–6238, 1980.

McGarr, A., Analysis of peak ground motion in terms of a model of inhomogeneous faulting, *J. Geophys. Res.*, *86*, 3901–3912, 1981.

McGarr, A., Scaling of ground motion parameters, state of stress and focal depth, *J. Geophys. Res.*, *89*, 6969–6979, 1984.

McGarr, A., and N. C. Gay, State of stress in the Earth's crust, *Annu. Rev. Earth Planet. Sci.*, *6*, 405–436, 1978.

McGarr, A., M. D. Zoback, and T. C. Hanks, Implications of an elastic analysis of in situ stress measurements near the San Andreas fault, *J. Geophys. Res.*, *87*, 7797–7806, 1982.

Meisling, K. E., and R. J. Weldon II, Slip-rate, offset, and history of the Cleghorn fault, western San Bernadino Mountains, southern California, *Geol. Soc. Am. Abstr. Programs*, *11*, 215, 1982.

Meisling, K. E., and R. J. Weldon II, Late cenozoic tectonics of the northwestern San Bernadino Mountains, southern California, *Geol. Soc. Am. Bull.*, *101*, 106–128, 1989.

Molnar, P., Continental tectonics in the aftermath of plate tectonics, *Nature*, *335*, 131–137, 1988.

Moos, D., and M. D. Zoback, Utilization of observations of well bore failure to constrain the orientation and magnitude of crustal stresses: Application to continental, Deep Sea Drilling Project and Ocean Drilling Project boreholes, *J. Geophys. Res.*, *95*, 9305–9325, 1990.

Morrow, C., and J. Byerlee, Permeability of rock samples from Cajon Pass, California, *Geophys. Res. Lett.*, *15*, 1033–1036, 1988.

Morrow, C., and J. Byerlee, Permeability of core samples from Cajon Pass Scentific drill hole: Results from 2100 to 3500 m depth, *J. Geophys. Res.*, this issue.

Morrow, C. A., L. Q. Shi, and J. D. Byerlee, Strain hardening and strength of clay-rich fault gouges, *J. Geophys. Res.*, *87*, 6771–6780, 1982.

Mount, V. S., and J. Suppe, State of stress near the San Andreas fault: Implications for wrench tectonics, *Geology*, *15*, 1143–1146, 1987.

Oldenburg, D. W., and J. Brune, Ridge transform fault spreading pattern in freezing wax, *Science*, *178*, 301–304, 1972.

Oldenburg, D. W., and J. N. Brune, An explanation for the orthogonality of ocean ridges and transform faults, *J. Geophys. Res.*, *80*, 2575–2585, 1975.

O'Neil, J. R., and T. C. Hanks, Geochemical evidence for water-rock interaction along the San Andreas and Garlock faults of California, *J. Geophys. Res.*, *85*, 6286–6292, 1980.

Oppenheimer, D. H., P. A. Reasenberg, and R. W. Simpson, Fault plane solutions for the 1984 Morgan Hill, California, earthquake sequence: Evidence for the state of stress on the Calaveras fault, *J. Geophys. Res.*, *93*, 9007–9026, 1988.

Paillet, F., and K. Kim, Character and distribution of borehole breakouts and their relationship to in situ stresses in deep Columbia river basalts, *J. Geophys. Res.*, *92*, 6223–6234, 1985.

Pezard, P. A., R. J. Weldon, R. N. Anderson, C. R. Wilkinson, and G. R. Ollier, Constraints on the geometrics of structures within the sedimentary rocks at the Cajon Pass scientific drillsite, California, *Geophys. Res. Lett.*, *15*, 965–968, 1988.

Pine, R. J., P. Ledingham, and C. M. Merrifield, In situ stress measurement in the Carnmenellis granite, II, Hydrofracture tests at Rosemanowes Quarry to depths of 2000 m, *Int. J. Rock Mech. Min. Sci.*, *20*, 63–72, 1983.

Plumb, R. A., and J. W. Cox, Stress directions in eastern North America determined to 4.5 km from borehole elongation measurements, *J. Geophys. Res.*, *92*, 4805–4816, 1987.

Raleigh, C. B., J. H. Healy, and J. D. Brederhoeft, Faulting and crustal stress at Rangely, Colorado, in *Flow and Fracture of Rocks*, *Geophys. Monogr. Ser.*, vol. 16, edited by H. C. Heard et al., pp. 275–284, AGU, Washington, D. C., 1972.

Ratigan, J., A statistical fracture mechanics determination of the apparent tensile strength in hydraulic fracturing, in *Hydraulic Fracturing Stress Measurements*, edited by M. D. Zoback and B. C. Haimson, pp. 159–166, National Academy Press, Washington, D. C., 1983.

Rummel, F., and J. Hansen, Interpretation of hydrofrac pressure recordings using a simple fracture mechanics simulation model, *Int. J. Rock Mech. Min. Sci. Geomech. Abstr.*, *26*, 483–488, 1989.

Rummel, F., J. Baumgärtner, and H. J. Alheid, Hydraulic fracturing stress measurements along the eastern boundary of the SW-German block, in *Hydraulic Fracturing Stress Measurements*, edited by M. D. Zoback and B. C. Haimson, pp. 3–17, National Academy Press, Washington, D. C., 1983.

Rummel, F., G. G. Mohring-Erdmann, and J. Baumgartner, Stress constraints and hydrofracturing stress data for the continental crust, *Pure Appl. Geophys.*, *124*, 875–895, 1986.

Saucier, F. J., E. D. Humphreys, and R. J. Weldon II, Stress near geometrically complex strike-slip faults: Application of the San Andreas fault at Cajon Pass, southern California, *J. Geophys. Res.*, this issue.

Schmitt, D. R., and M. D. Zoback, Poroelastic effects in the determination of the maximum horizontal principal stress in hydraulic fracturing tests: A proposed breakdown equation employing a modified effective stress relation for tensile failure, *Int. J. Rock Mech. Min. Sci.*, *26*, 499–506, 1988.

Schmitt, D. R., and M. D. Zoback, Pore pressure effects in tensile rupture of low porosity rocks: Possible evidence for dilatancy hardening, *Eos Trans. AGU*, *71*, 1586, 1990.

Shamir, G., Crustal stress orientation profile to a depth of 3.5 km near the San Andreas fault at Cajon Pass, California, Ph.D. thesis, Stanford Univ., Stanford, Calif., 1990.

Shamir, G., and M. D. Zoback, Stress orientation profile to 3.5 km depth near the San Andreas fault at Cajon Pass, California, *J. Geophys. Res.*, this issue.

Sibson, R. H., Frictional constraints on thrust, wrench and normal faults, *Nature*, *249*, 542–544, 1974.

Sibson, R. H., Fault zone models, heat flow, and the depth distribution of earthquakes in the continental crust of the United States, *Bull. Seismol. Soc. Am.*, *72*, 151–163, 1982.

Sibson, R. H., Continental fault structure and the shallow earthquake source, *J. Geol. Soc. London*, *140*, 741–767, 1983.

Sieh, K. E., Prehistoric large earthquakes produced by slip on the San Andreas fault at Pallet Creek, California, *J. Geophys. Res.*, *83*, 3907–3939, 1978.

Sieh, K., M. Stuiver, and D. Brillinger, A more precise chronology of earthquakes produced by the San Andreas fault in southern California, *J. Geophys. Res.*, *94*, 603–623, 1989.

Silver, L. T., and E. W. James, Geologic setting and lithologic colum of the Cajon Pass deep drill hole, *Geophys. Res. Lett.*, *15*, 941–944, 1988*a*.

Silver, L. T., and E. W. James, Lithologic column of the Arkoma drill hole and its relation to the Cajon Pass deep drill hole, *Geophys. Res. Lett.*, *15*, 945–948, 1988*b*.

Smith, R. B., and R. L. Bruhn, Intraplate extensional tectonics of the Eastern Basin-Range: Inferences on structural style from

seismic reflection data, regional tectonics, and thermal-mechanical models of brittle-ductile transition, *J. Geophys. Res.*, *89*, 5733–5762, 1984

Solomon, S. C., E. A. Bergman, W. S. D. Wilcock, and G. M. Purdy, On the state of stress near oceanic transforms and fracture zones, *Eos Trans. AGU*, *70*, 469, 1989.

Stephansson, O. (Ed.), *Proc. of International Symposium on Rock Stress and Rock Stress Measurements, Stockholm, 1–3 September, 1986*, 694 pp., Centek, Lulea, Sweden, 1986.

Stock, J. M., and J. H. Healy, Stressfield at Yucca Mountain, Nevada, in Geologic and Hydrologic Investigations of a Potential Nuclear Waste Disposal Site at Yucca Mountain, Southern Nevada, *U.S. Geol. Surv. Bull.*, *87-93*, 1988.

Stock, J. M., J. H. Healy, S. H. Hickman, and M. D. Zoback, Hydraulic fracturing stress measurements at Yucca Mountain, Nevada, and the relationship to the regional stress field, *J. Geophys. Res.*, *90*, 8691–8706, 1985.

Tsukahara, H., Stress measurements utilizing the hydraulic fracturing technique in the Kanto-Tokai area, Japan, in *Hydraulic Fracturing Stress Measurements*, edited by M. D. Zoback and B. C. Haimson, pp. 143–148, National Academy Press, Washington, D. C., 1983.

Vernik, L., and A. Nur, Petrophysical analysis of the Cajon Pass scientific well: Implications for fluid flow and seismic studies in the continental crust, *J. Geophys. Res.*, this issue.

Vernik, L., and M. D. Zoback, Effects of rock elastic and strength properties in estimation of the state of stress at depth, in *Rock at Great Depth*, edited by V. Maury and D. Fourmaintraux, pp. 1033–1040, A. A. Balkema, Rotterdam, Netherlands, 1989.

Vernik, L., and M. D. Zoback, Strength anisotropy of crystalline rock: Implications for assessment of in situ stresses from wellbore breakouts, in *Rock Mechanics Contributions and Challenges*, edited by W. Hustrulid and G. Johnson, pp. 841–848, A. A. Balkema, Rotterdam, Netherlands, 1990.

Vernik, L., and M. D. Zoback, Estimation of maximum horizontal principal stress magnitude from stress-induced well bore breakouts in the Cajon Pass scientific research borehole, *J. Geophys. Res.*, this issue.

Vincent, P., and P. L. Ehlig, Laumontite mineralization in rocks exposed north of San Andreas fault at Cajon Pass, southern California, *Geophys. Res. Lett.*, *15*, 977–980, 1988.

Warren, W. E., and C. W. Smith, In situ stress estimates from hydraulic fracturing and direct observation of crack orientation, *J. Geophys. Res.*, *90*, 6829–6839, 1985.

Webb, T. H., and H. Kanamori, Earthquake focal mechanisms in the eastern Transverse Ranges and San Enigdio Mountains, southern California and evidence for a regional decollement, *Bull. Seismol. Soc. Am.*, *75*, 737–757, 1985.

Weibols, G. A., and N. G. W. Cook, An energy criterion for the strength of rock in polyaxial compression, *Int. J. Rock Mech. Min. Sci.*, *5*, 529–549, 1968.

Weldon, R. J., The late Cenozoic geology of Cajon Pass: Implications for tectonics and sedimentation along the San Andreas fault, Ph.D. thesis, 400 pp., Calif. Inst. of Technol., Pasadena, 1986.

Weldon, R. J., and K. E. Sieh, Holocene rate of slip and tentative recurrence interval for large earthquakes on the San Andreas fault, Cajon Pass, southern California, *Geol. Soc. Am. Bull.*, *96*, 793–812, 1985.

Weldon, R. J., and J. E. Springer, Active faulting near the Cajon Pass well, southern California; Implications for the stress orientation near the San Andreas fault, *Geophys. Res. Lett.*, *15*, 993–996, 1988.

Wicklund, A. P., R. Andrews, and R. Johnson, Drilling summary, Cajon Pass scientific drilling project: Phase I, *Geophys. Res. Lett.*, *15*, 937–940, 1988.

Wicklund, A. P., R. S. Andrews, G. A. Barber, and R. J. Johnson, Cajon Pass scientific drilling project: Drilling overview, in *Super-Deep Continental Drilling and Deep Geophysical Sounding*, edited by K. Fuchs, Y. A. Kozlovsky, A. J. Krivtsov, and M. D. Zoback, pp. 40–56, Springer-Verlag, New York, 1990.

Wilcock, W. S. D., G. M. Purdy, and S. C. Solomon, Microearthquake evidence for extension across the Kane transform fault, *J. Geophys. Res.*, *95*, 15,439–15,462, 1990.

Wong, I., Seismotectonics of the Coast Ranges in the vicinity of Lake Berryessa, northern California, *Bull. Seismol. Soc. Am.*, *80*, 935–950, 1990.

Zemanek, J., E. E. Glenn, Jr., L. J. Norton, and R. L. Caldwell, Formation evaluation by inspection with the borehole televiewer, *Geophysics*, *35*, 254–269, 1970.

Zoback, M. D., and B. C. Haimson (Eds.), *Workshop on Hydraulic Fracturing Stress Measurements*, pp. 44–54, U.S. National Committee for Rock Mechanics, National Academy Press, 1983.

Zoback, M. D., and J. H. Healy, Friction, faulting and in situ stress, *Ann. Geophys.*, *2*, 689–698, 1984.

Zoback, M. D., and S. Hickman, In situ study of the physical mechanisms controlling induced seismicity at Monticello Reservoir, South California, *J. Geophys. Res.*, *87*, 6959–6974, 1982.

Zoback, M. D., H. Tsukahara, and S. Hickman, Stress measurements at depth in the vicinity of the San Andreas fault: Implications for the magnitude of shear stress at depth, *J. Geophys. Res.*, *85*, 275–284, 1980.

Zoback, M. D., D. Moss, L. Mastin, and R. N. Anderson, Well bore breakouts and in situ stress, *J. Geophys. Res.*, *90*, 5523–5530, 1985.

Zoback, M. D., et al., New evidence on the state of stress of the San Andreas fault system, *Science*, *238*, 1105–1111, 1987.

Zoback, M. D., J. Baumgärtner, and D. Moos, Hydraulic fracturing stress measurements in the Moodus, Conn. research borehole and shallow earthquakes, *Eos Trans. AGU*, *69*, 491, 1988*a*.

Zoback, M. D., L. T. Silver, T. Henyey, and W. Thatcher, The Cajon Press scientific drilling project: Overview of phase I, *Geophys. Res. Lett.*, *15*, 933–936, 1988*b*.

Zoback, M. L., and M. D. Zoback, State of stress in the conterminous U.S., *J. Geophys. Res.*, *85*, 6113–6156, 1980.

Zoback, M. L., and M. D. Zoback, Tectonic stress field of the continental U.S., in Geophysical Framework of the Continental United States, edited by L. Pakiser and W. Mooney, *Mem. Geol. Soc. Am.*, *172*, 523–539, 1989.

Zoback, M. L., et al., Global patterns of tectonic stress, *Nature*, 341, 291–298, 1989.

J. H. Healy, Office of Earthquakes, Volcanoes and Engineering, U.S. Geological Survey, Menlo Park, CA 94025 (Tel. 415-329-4848; FAX 415-329-5163).

M. D. Zoback, Department of Geophysics, Stanford University, Stanford, CA 94305 (Tel. 415-723-4746; FAX 415-725-7344).

(Received November 29, 1990;
revised June 24, 1991;
accepted July 24, 1991.)